This manuscript is a non-peer reviewed preprint. The preprint was submitted to MARINE GEOLOGY for review and is currently in review. Subsequent version of this manuscript may have slight differences.

Foraminifera as a tool for the reconstruction of paleobathymetry and geohazard: A case study from Taiwan

Raúl Tapia [1*], Sicheng Le [1], Sze Ling Ho [1*], Maria-Angela Bassetti [2], In-Tian Lin [3], Hui-Ling Lin [4], Yuan-Pin Chang [4], Kuo-Tung Jiann [4], Pei-Ling Wang [1], Jheng-Kuan Lin [1], Nathalie Babonneau [5], Gueorgui Ratzov [6], Shu-Kun Hsu [7], Chih-Chieh Su [1*]

1 Institute of Oceanography, National Taiwan University, No. 1, Sec. 4, Roosevelt Road 10617 Taipei, Taiwan

2 CEFREM-UMR 5110, Université de Perpignan Via Domitia, 52 Avenue Paul Alduy, 66860 Perpignan cedex, France

3 Exploration and Development Research Institute, CPC Corporation, Miaoli 36042, Taiwan

4 Department of Oceanography, National Sun Yat-sen University, Kaohsiung 80424, Kaohsiung, Taiwan

5 UMR GEO-OCEAN, Univ Brest, CNRS, Ifremer, IUEM, 29280 Plouzané, France

6 Université Côte d'Azur, CNRS, Observatoire de la Côte d'Azur, IRD, Géoazur, Nice, France

7 Department of Earth Sciences, National Central University, Taiwan

* Corresponding author: Raúl Tapia (raultapia@ntu.edu.tw); Sze Ling Ho (slingho@ntu.edu.tw); Chih-Chieh Su (donccsu@ntu.edu.tw).

ABSTRACT

The calcite tests of foraminifera are an important biogenic component of marine sediments. The abundance of foraminiferal tests in marine sediments broadly varies with bathymetry, thus has been used to reconstruct paleobathymetry. It is also promising as a tracer for downslope transport triggered by earthquakes and typhoons, especially if the displaced material from shallow locality contrasts strongly with the background autochthonous sediments in terms of foraminiferal abundance, such as the ratio of benthic and planktic foraminifera termed %P. However, its applicability in sediments off Taiwan has not been assessed. Taiwan is located in the path of typhoons and at tectonic plate margins, where typhoons and earthquakes may trigger submarine geohazards. This, combined with the fact that its seafloor spans a large bathymetric range, render this region an ideal natural laboratory to evaluate the applicability of %P as a proxy for tracing submarine geohazards and bathymetry. Here we report foraminiferal abundance, %P, grain size and elemental data from 148 surface sediment samples off 6 sectors off Taiwan, namely Southern Okinawa Trough, Hoping-Nanao-Hateruma Basins, Taitung-Hualien, Hengchun Ridge, Gaoping, and Changyun Sand Ridge. Of all the hydrographic and sedimentological parameters assessed, seafloor bathymetry is the major driver of foraminiferal abundance and %P in these regions. Notably, several data points deviate from the regional %P-water depth relationship. Based on sedimentological parameters and previous studies, we posit that these outliers may have to do with local sedimentation setting. These processes include earthquake-induced sediment transport via submarine canyon in the Southern Okinawa Trough, typhoon-triggered sediment flushing in Gaoping Canyon, cross-shelf and northward advection of planktic foraminifera on the Gaoping shelf, and carbonate dissolution in deep Hateruma Basin. Off Taiwan, the %P value in sediments increases exponentially with bathymetry (R^2 = 0.72), and agrees well with the global calibration obtained by combining 827 data from several regions of the global ocean. The regional %P-water depth relationship may be useful for reconstructing paleobathymetry here, albeit with an uncertainty of ~400 m that increases with bathymetry especially >2000 m. Our results also highlight the potential of the %P index as a tracer for downslope transport and lateral advection in the water column. The downcore application of %P therefore has the potential to reconstruct past geohazard events while also identify autochthonous sediment sequences that are suitable for paleoceanographic reconstruction.

Keywords: Foraminifera, %P, paleobathymetry, downslope sediment transport, geohazard, Taiwan

INTRODUCTION

The calcite tests of foraminifera are a major biogenic component of marine sediments. The displacement of foraminiferal tests after deposition may occur as an outcome of submarine sediment density flow events such as turbidity currents, debris flows, hyperpycnal plumes, and submarine landslides (Schmuker, 2000). Thus, the study of foraminiferal tests in sediments, alongside grain size, mineralogy composition, and organic carbon content analysis, are the primary tools in the identification of mass sediment transport events in the sedimentary record (Jones, 2013). Each of the aforementioned approaches are highly complementary. Although they can be applied separately, they afford a more comprehensive picture of the sedimentation process when used in tandem.

Contrasting displaced foraminifera with modern autochthonous fauna allows the identification of the sedimentary source (original depth of deposition) and the inference of transport processes (Ash-Mor et al., 2017; Ash-Mor et al., 2021; Usami et al., 2017). The inclusion of gravitationally displaced individuals allochthonous fauna in the autochthonous foraminiferal assemblage from deeper part of the basins will alter the diversity and dominance parameters of the local fauna (Hayward et al., 2019; Schröder-Adams et al., 2008). Furthermore, during highly dynamic downslope transport, foraminiferal tests can be subjected to size sorting, abrasion, fragmentation, or dissolution (thinner shelled calcareous tests) when deposited close to or below the calcite compensation depth (Hayward et al., 2019; Schröder-Adams et al., 2008; Sugawara et al., 2009; Uchida et al., 2010). These changes in foraminiferal parameters caused by sediment transport may thus complement the information obtained from traditional sedimentological approaches. In fact, benthic foraminiferal assemblages have been used to trace turbidites and other types of debris flows, as well as paleobathymetric reconstructions in deep geological time (Jones, 2013). In contrast to mineralogical composition and grain size approaches where the observed data are driven exclusively by physical or chemical processes, the use of foraminifera to interpret sediment transport processes requires additional considerations, as environmental parameters may also influence foraminiferal distribution (van der Zwaan et al., 1990). Therefore, understanding the living environmental conditions of the organism and their modern distribution in sediments is a prerequisite to downcore applications (Gooday, 2003; Jones, 2013; van der Zwaan et al., 1999).

Taiwan is prone to natural geohazards linked to climate (e.g., tropical cyclones) and tectonics (e.g., earthquakes). These so-called extreme events can cause enormous damage to public infrastructure, private property, and fatalities. A less recognized aftershock of these natural hazards is their ability to generate turbidity currents and gravity flows on the seafloor. Therefore, Taiwan is an ideal natural laboratory to study the impact of submarine sediment density flows on the distribution of foraminiferal tests in sediments.

To date, foraminiferal studies off Taiwan have been mostly focusing on the temporal flux in the water column (i.e., sediment traps), benthic foraminiferal biocenosis (Lin and Hsieh, 2007; Lin, 2014; Lin et al., 2011), and the application of benthic foraminifera to assess coral reef health (Chen and Lin, 2017). Little attention has been paid to the utility of foraminifera as a tracer for geohazards or extreme events, despite promising early observations that suggested a correlation between the transport of foraminiferal tests and the landfall of typhoons (Lin et al., 2005).

The main objective of this study is to assess the applicability of foraminiferal indices, with emphasis on the percentage of planktic foraminifera (%P), as a tracer of sediment transport in response to extreme events such as typhoons and earthquakes. To this end, we mapped the spatial distribution of foraminiferal indices in surface sediments off Taiwan spanning a large bathymetric range (Fig. 1a). Our approach is based on the ecology of foraminifera, that is, the relationship between bathymetry and the distribution of planktic and benthic foraminifera (Berger and Diester-Haass, 1988; Gibson, 1989; Hayward and Triggs, 2016; Hayward et al., 2019; Jones, 2013; Nigam and Henriques, 1992; Schmuker, 2000; van der Zwaan et al., 1999, 1990; van Hinsbergen et al., 2005). This approach implies that deviations from the main bathymetry-foraminifera relationship reflect “anomalies” in the depositional environment due to processes like downslope transport of sediment. Whilst seemingly straightforward, the accuracy of this approach requires further scrutiny as this relationship varies from region-to-region (van der Zwaan et al. 1990). To better constrain the bathymetry-foraminifera relationship off Taiwan, we used grain size and organic carbon content to cross-evaluate the likelihood that the collected sediments have been tampered by sediment transport processes. We also assessed if the foraminiferal indices in our study region change in response to environmental parameters other than water depth, e.g., seawater temperature, salinity, and water fertility.

1.1 Modern climate, oceanography and geological setting of study area

The upper ocean circulation around Taiwan is dominated by the warm Kuroshio Current that originates in the equatorial Pacific. At the Luzon Strait, a minor branch of this nutrient-deficient current splits in the direction of the South China Sea and flows along the southern part of Taiwan toward the Taiwan Strait (Fig. 1b). The upper circulation in the Taiwan Strait is primarily controlled by the Taiwan Warm Current, which consists of waters from the South China Sea and the Kuroshio branch, and flows towards the East China Sea all year round. In winter, the East China Sea Coastal Current (ECSCC) flowing towards the South China Sea can be observed in the Taiwan Strait (Fig. 1b) (Huang et al., 2015; Liang et al., 2003). The main branch of the Kuroshio Current flows northward along the eastern flank off Taiwan, crossing the Ilan Ridge at the Yonaguni Depression toward the East China Sea (Fig. 1b). The continental shelf to the north of the Okinawa Trough creates a topographic constriction for the Kuroshio Current, prompting the formation of eddies that actively capture and retain suspended sediments on the shelf. The shelf sediments are subsequently delivered downslope into the Okinawa Trough via submarine canyons such as the Mien-Hua Canyon (Chiang et al., 2022).

Taiwan is particularly prone to seismic activity due to its location at the margin of the Philippine Sea and Eurasian plates that collide at a rate of 8 cm yr^{-1} (Lehu et al., 2015; Su et al., 2012). Seismic activity concentrates along the eastern coast of Taiwan and along the east-west axis of the Southern Okinawa Trough. In the past 22 years, 23 ≥ 6.5 MW earthquakes have occurred here (Seismological Center – Republic of China, 2022). Such active seismic activity shapes the seafloor morphology by facilitating the supply of material downslope via gravity flows (Huh et al., 2004; Lee et al., 2004).

In addition, Taiwan is also marked by frequent occurrence of tropical cyclones (known locally as typhoons) (Water Resources Agency – Republic of China, 2022). Although tropical cyclones may occur throughout the year, they are most severe during May to October, which drives a marked seasonality in precipitation patterns as >75 % of annual rainfall, on average >2500 mm

y^{-1}, occurs during late summer and early autumn (Water Resources Agency – Republic of China, 2022). Typhoons, usually accompanied by strong winds and heavy rains, can in some cases deliver as much rain as the total amount during a normal year. These short-lived episodes of heavy rain increase runoff and sediment load delivered by the river system to coastal waters around Taiwan (Chien and Kuo, 2011; Lee et al., 2015). For example, the Morakot typhoon (2009) delivered an accumulated 3000 mm of rainfall within a time window of 4 days with a peak of 500 to 800 mm in 24 hours (Chien and Kuo, 2011), which led to over 12000 landslides and extensive flooding in southern Taiwan. As a result of the heavy rains during the Morakot typhoon, a large amount of sediment was removed and transported, leading to the increase in runoff and sediment load of the Gaoping River in southern Taiwan, from its long-term annual averages of <1000 m s^{-1} and ~23 Mt to ranges of 3800–~27000 m s^{-1} and 450–700 Mt (Lee et al., 2015). The excessive discharge of sediment led to the development of several sediment gravity flows that damaged the submarine cables downstream of the Gaoping Submarine Canyon (Su et al., 2012). The Gaoping Submarine Canyon stretches for 260 km covering a bathymetric range from 80 m to 3400 m water depth and serves as a channel to deliver terrigenous materials and carbon into the South China Sea. Substantially smaller, the Fangliao Submarine Canyon stretches for 60 km across the continental slope of the Gaoping sector and connects with the lower section of the Gaoping Submarine Canyon (Fig. 1) (Su et al., 2012).

2. MATERIALS AND METHODS

Surface sediment samples (n=148) analyzed in this study (Fig. 1a, 1c and 1d) were collected during several oceanographic cruises carried out between 2002 and 2018 on board of Taiwanese vessels R/Vs Ocean Researcher 1, 2, 3 and New Ocean Researcher 1, as well as French vessel R/V Marion Dufresne. Samples were retrieved using various gears, including sediment grab, box corer, and gravity corer, from water depths ranging from 13 to 5714 m (see Table S1 for details). Study sites were grouped into two main geographical areas, namely (1) East Taiwan (>121º E; n = 85) and (2) West Taiwan (<121º E; n = 63) (Fig. 1a). East Taiwan is comprised of sites in the Southern Okinawa Trough, Hoping-Nanao-Hateruma Basins, and

Taitung-Hualien Slope, while West Taiwan is comprised of Hengchun Ridge, Changyun Sand Ridge, and Gaoping sector (Fig. 1a).

>> Figure 1<<

2.1 Sediment sample processing

Surface sediment samples were freeze- dried, weighed, and subsampled for foraminiferal and geochemical analyses. In the case of insufficient material for both analyses, we prioritized micropaleontological analysis. The subsamples for foraminiferal analysis were wet-sieved through a sieve of 63 µm open mesh, and the remnant was dried at low temperature (50 ºC) and weighed.

2.2 Foraminifera recovery and associated indices

Sediment samples (>63 µm) were dry-sieved through sieves of 125 and 250 µm open mesh. The size fraction of 63–125 µm was not considered in this study because of two reasons. First, as previous work has shown, the faunal composition (e.g., bathymetric group) is similar for the small size fraction (63–125 µm) and the size fraction >125 µm (Hayward et al., 2019). Second, the small size fraction (63–125 µm) usually contains a large proportion of juvenile forms that are problematic to identify, and its recovery is extremely time consuming (Schröeder et al., 1987). The small size fraction was stored for future studies. The census count only considered intact planktic and benthic foraminiferal tests. The abundance was calculated for each sample and presented as the number of organisms per gram of dry sediment (ind. g^{-1}) for the size fraction of >125 µm. The percentage of planktic foraminifera (%P) is defined as the ratio of planktic foraminiferal tests in the total pool of foraminiferal tests in the sediment, and is calculated as follows:

$$\%P = P / (P+B) * 100$$

where P is the number of specimens of planktic foraminifera and B is the number of specimens of benthic foraminifera. Following Hayward et al (2019), only samples with at least 50 specimens were considered for the calculation of %P.

2.3 Geochemical and sedimentological parameters

2.3.1 Elemental analysis

The Total Organic Carbon (TOC) and Total Nitrogen (TN) contents were measured in three laboratories with slightly different methodologies. The samples measured in the Institute of Oceanography (NTU) were decalcified using 2N hydrochloric acid (HCl, aq), dried at 50 °C, and measured using an Vario MICRO CUBE (Elementar) Elemental Analyzer. Samples measured in National Sun Yat-sen University were decalcified using phosphoric acid (10%) and measured using an Analytic Jena Multi N/C 2100 Elemental Analyzer. The samples measured in the Department of Geoscience (NTU) were decalcified using 3N hydrochloric acid (HCl, aq), freeze-dried and measured using a Flash EA 1112 Elemental Analyzer. The overall relative error of TOC and TN measurements was less than 5% based on replicate analysis. The C/N ratio was computed as the molar ratio between TOC and TN.

2.3.2 Grain size analysis

Grain size analysis was carried out in the Environmental Radioactivity & Sedimentology Laboratory (IONTU) using a Beckman Coulter LS13 320 Laser Diffraction Particle Analyzer with a measurement range of 0.375–2000 µm. All samples were pretreated following the protocol of Poppe et al (2000). Briefly, carbonates were removed using 10% hydrochloric acid (HCl). Carbonate-free samples were then treated with 15% hydrogen peroxide (H_2O_2) for 1 to 2 days to remove organic matter. Ultrasonic devices and sodium hexametaphosphate ($Na(PO_3)_6$) were used to deflocculate and disperse sediment grains prior to grain size analysis. Relative abundances in percentage of clay (<4 µm), silt (4–63 µm) and sand (>63 µm) were calculated from the grain size data of bulk sediment.

2.4 Data treatment and statistical analyses of environmental data

Water temperature, salinity, fluorescence, and dissolved oxygen data collected during the last 11.5 years (March 2004 to September 2015) were requested from Ocean Data Bank (ODB) of the Ministry of Science and Technology – Republic of China (2022) to examine environmental control on the spatial distribution of foraminiferal abundance and its associated indicators.

To improve the spatial representativeness of spatially sparse and inhomogeneous hydrographic data, the ODB data set was first gridded and then each sediment site was matched to the closest ODB data grid for the extraction of the hydrographic data. The hydrographic data were then averaged to obtain the mean annual value for each parameter. Sparse temporal sampling of this dataset does not allow a meaningful calculation of monthly average.

The hydrographic parameters were grouped into surface and bottom conditions. Surface condition was defined as 0–400 m water depth. We selected this water depth range because most of the planktic foraminifera species live within this range (Schiebel and Hemleben 2017 and references therein). Meanwhile, bottom condition corresponds to the data closest to the seafloor as an approximation of the bottom water conditions influencing benthic foraminifera that live on/in the sediment. Specifically, we used the average values of the last 10 m, 50 m, 100 m, and 500 m of the water column for stations located in <100 m, 100–500 m, 500–1000 m and 1000–2500 water depth, respectively. In the case of stations located below 2500 m water depth we averaged the data from 2500–3500 m of the water column. Statistical analyses including correlation coefficients were performed using statistical software PAST 4.09 (PAleontological STatistics) (Hammer et al., 2001).

3. Results

3.1 Correlation between foraminifera and environmental parameters

Correlation coefficients between foraminiferal indices (%P, planktic, and benthic foraminiferal abundance) and environmental parameters, including bulk sediment data (%Sand and TOC content) and hydrographic data (temperature, salinity, fluorescence, dissolved oxygen), are presented in Table 1. The correlations between planktic foraminiferal and environmental parameters of the upper water column (0–400 m) are relatively weak ($R < 0.36$), with the strongest correlation observed for fluorescence and water depth. Of all parameters, benthic foraminiferal abundance shows the strongest correlation with water depth ($R = -0.65$), and weaker but statistically significant correlations with parameters related to food availability i.e., fluorescence ($R = 0.25$), TOC ($R = -0.39$) and bottom water oxygen content ($R = 0.42$). %P derived from the ratio of planktic and benthic foraminiferal abundances, on the other hand, shows in general stronger relationships with environmental parameters. Of all the variables, the strongest correlation is found between water depth and %P (R = 0.57). %P is more strongly correlated to planktic foraminiferal abundance (R = 0.76) than to benthic foraminiferal abundance (R = -0.48). Parameters associated with ocean productivity show relatively weak correlations with %P and in opposite directions; fluorescence and bottom water dissolved oxygen correlate negatively with %P (R = -0.49 for fluorescence and R = -0.35 for bottom water dissolved oxygen) while the TOC correlates positively with %P (R = 0.26) (Table 1).

>>Table 1<<

3.2 Abundance of benthic foraminifera in surface sediments off Taiwan

The abundance of benthic foraminifera at sites off Taiwan ranges from 0 to 169 ind. g^{-1}, with a median value of ~5 ind. g^{-1} (orchid boxplot in Fig 2a). The median abundance of benthic foraminifera varies by region, ranging from ~1 to ~10 ind. g^{-1} (Fig. 2a). The highest abundance is observed in the Changyun Sand Ridge (~10 ind. g^{-1}), while the lowest abundances occur in Taitung-Hualien (~3 ind. g^{-1}) and Hoping-Nanao-Hateruma Basins (~1 ind. g^{-1}). Meanwhile, intermediate abundances are observed in the Gaoping (~7 ind. g^{-1}), Southern Okinawa Trough (~6 ind. g^{-1}), and Hengchun Ridge (~6 ind. g^{-1}).

When considered by site, the spatial distribution of benthic foraminifera (Fig. 2e) is characterized by high abundance off Changyun Sand Ridge, Gaoping, Hengchun Ridge and several Southern Okinawa Trough sites near the Ryukyu Arc. Notably, the highest abundance of benthic foraminifera of the entire dataset occurs in the Southern Okinawa Trough (169 ind. g^{-1}) (Fig. 2e). Most samples from the Hoping-Nanao-Hateruma Basins and Taitung-Hualien contain relatively low abundance of benthic foraminifera (Fig. 2a and 2e). Benthic foraminiferal abundance broadly decreases with increasing water depth (Fig. 2c), with some spatial variability within the Gaoping and Southern Okinawa Trough (Fig. 2c and 2e). In the Gaoping sector, samples from Gaoping Submarine Canyon show relatively low benthic foraminiferal abundance compared to samples from a similar bathymetric range off Southwestern Taiwan (Fig. 2c and S1). Meanwhile, samples from the Southern Okinawa Trough show a large range of benthic foraminiferal abundance for a narrow range of bathymetry between 1500–2000 m (Fig. 2c).

>> Figure 2 <<

3.3 Abundance of planktic foraminifera in surface sediments off Taiwan

The planktic foraminiferal abundances off Taiwan range from 0 to ~1000 ind. g^{-1}, with a median value of ~14 ind. g^{-1} (orchid boxplot in Fig 2b). The planktic foraminiferal abundance varies substantially by region, with extremely low to no presence in the Changyun Sand Ridge. The highest abundance occurs in the Hengchun Ridge sector (~155 ind. g^{-1}), while intermediate to low abundances occur in the Taitung-Hualien (~27 ind. g^{-1}), Hoping-Nanao-Hateruma Basins (~23 ind. g^{-1}), Gaoping (~15 ind. g^{-1}) and Southern Okinawa Trough (~11 ind. g^{-1}) sectors (Fig. 2b).

When considered by site, the spatial distribution of planktic foraminifera shows an increase in abundance with increasing water depth (Fig. 2d and 2f), more obvious off West Taiwan (e.g., Gaoping sector) than off East Taiwan. There is substantial scatter in the data from Gaoping sector as planktic foraminiferal abundances are anomalously low in the sediments of submarine canyons compared to the rest of the Gaoping dataset, thereby forming two separate clusters in the scatter plot (Fig. 2d). The Southern Okinawa Trough and Hoping-Nanao-Hateruma Basins samples show a large spread in planktic foraminiferal abundances within a small bathymetric range (Fig. 2d). Interestingly, the planktic foraminiferal abundance in Hoping-Nanao-Hateruma Basins appears to decrease sharply with water depth (R2 = 0.8; exponential fit), in the opposite direction of the overall regional relationship between planktic foraminiferal abundance and bathymetry. Due to the larger scatter in the dataset (Fig. 2d), the overall correlation between water depth and planktic foraminiferal abundance is weaker than that for benthic foraminiferal abundance (Table 1).

>> Figure 3 <<

3.4 Planktic foraminiferal percentage (%P) off Taiwan

Out of 119 samples, only 88 (67) samples yield >50 (>100) individuals of benthic and planktic foraminifera (Fig. 3a). Both sets of data (>50 and >100) yield comparable regressions with similarly good fit (Fig. 3a; discussion in Section 4.2). In the following, we consider only samples containing >50 counts for our results and discussion of %P (Section 2.2). Fig. 3 shows the spatial distribution of %P off Taiwan, which is in the range of 0 and 99.8 % (Fig. 3b and 4a). In general, as expected the %P value in the sediments off Taiwan increases with increasing water depth (R^2 = 0.73; exponential model) (Fig. 4a). %P values in the Changyun Sand Ridge and Hengchun Ridge sectors off West Taiwan generally follow the regional trend of %P and water depth (Fig. 4a). Compared to these sectors, larger scatter, and variability (within a bathymetric range) can be observed in the Southern Okinawa Trough and Gaoping sectors, even though on average %P values in these sectors do increase with increasing water depth (Fig. 4a). The scatter in these datasets is evident as data points that lie outside the 95% prediction bounds of the regression are mostly from these two sectors in addition to one site from Hoping-Nanao-Hateruma Basins (Fig. 4a). Data dispersion in these sectors is further depicted using boxplots grouped by depth-bin (Fig. 4b). Interestingly, the largest data dispersion in each sector seems to be associated with a particular bathymetric range, i.e., 0–500 m depth for Gaoping sector, 1000–1500 m depth for Southern Okinawa Trough region and 3000–4000 m depth for Hoping-Nanao-Hateruma Basins (Fig. 4b).

>> Figure 4 <<

3.5 Grain size and bulk geochemistry

In our sediment collection, silt is the dominant size class with a mean contribution of ~65% (Fig 5a). The clay and sand size classes are less abundant with a mean value of 17% and 18%, respectively. The spatial distribution of sand/silt/clay size classes differs between the designated regions of East and West Taiwan (Fig. 5b and 5c). Fine-grained size classes (i.e., clay and silt) dominate the regions in East Taiwan (Fig. 5b), while West Taiwan is marked by a larger presence of coarser sand fraction (Fig. 5c). Overall, the sand content decreases with increasing water depth.

In West Taiwan, the “sandy” sediments are mostly restricted to the Changyun Sand Ridge (< 50 m; see Fig. 1) and mostly the shelf (< 200 m) of the Gaoping sector or close to the mouth of the Gaoping River, while in East Taiwan coarser sediments are restricted to the area influenced by the Lanyang River in the Southern Okinawa Trough (Fig. 5b and S1). In the deep Hoping-Nanao-Hateruma Basins, the surface sediments are mainly composed of silt and clay, but the sand content can be as high as 7% at a few sites (Fig. 5b).

The TOC content and C/N ratios are relatively low in most sediments off Taiwan (Fig. 5d-g), with median values of 0.7 wt% and ~6, respectively (Fig. 5d and 5e). Samples from the Changyun Sand Ridge contain the lowest TOC content. The lowest C/N ratios are found in the Gaoping sector, while the highest TOC content and C/N ratio were observed in the Southern Okinawa Trough (Fig. 5d and 5e). The overall low C/N ratios in the surface sediments (<10) indicate that the organic matter in these sediments is predominantly marine in origin. The exception to this trend is two stations in the Southern Okinawa Trough with TOC content and C/N values >1.9 wt% and >15, respectively, substantially higher than the rest of the dataset (Fig. 5d and 5e). Both TOC content and C/N ratio show statistically significant correlation ($p < 0.05$) with water depth (Fig. 5d and e), with $R^2 = 0.38$ for C/N ratio and $R^2 = 0.69$ for TOC.

>> Figure 5 <<

4. Discussion

4.1 Assessing potential bias on %P value due to low foraminiferal counts

To the best of our knowledge, there is no consensus in the literature concerning the minimum foraminiferal tests (counts) needed for a robust interpretation of %P. Most studies advocate the use of at least 100 tests for the census count, up to as high as 500 (Gibson, 1989; Nigam and Henriques, 1992; Schmuker, 2000; van der Zwaan et al., 1990; van Hinsbergen et al., 2005; van Marle et al., 1987). In this study, due in part to the small sample size, it was not always possible to reach 100 tests per sample for census count. We note that Hayward et al (2019) recently demonstrated that census counts based on >50 tests yield robust results for %P distribution in sediments off New Zealand. To evaluate if this is also true for our %P dataset, we compared data based on census count >50 and >100 counts (Fig. 3a). We do not observe any systematic offset between these two datasets. Furthermore, the regression lines based on data with >50 counts and >100 counts show a similar relationship with comparable R^2 values (R^2 of >50 counts = 0.72, R^2 of >100 counts = 0.70), suggesting that including %P data based on >50 counts in our Taiwan dataset does not bias the %P values nor the relationship between %P and water depth, in agreement with the results from New Zealand (Hayward et al., 2019).

4.2 Environmental controls on foraminiferal abundance and %P

Previous studies have suggested that %P in marine sediments may be influenced by regional hydrography, such as the spatial extension of the monsoonal upwelling (van Marle et al., 1987) and land-sea salinity gradients (Nigam and Henriques, 1992). To assess the influence of hydrographic variables on foraminiferal abundance off Taiwan, we examine the correlation between foraminiferal indices (foraminiferal abundance and %P) and hydrographic data (surface and bottom) as well as bathymetry (Table 1). Our results show that %P has the strongest correlation with water depth (bathymetry) among all environmental variables, as expected, suggesting that off Taiwan the water depth of depositional setting exerts the strongest control on %P, hinting at its potential as a proxy for paleobathymetric reconstruction.

Ocean productivity (i.e., fluorescence and TOC) and bottom water oxygen content are considered relevant drivers of foraminiferal ecology (Gooday, 2003; Schiebel and Hemleben, 2017). In the case of planktic foraminifera, high ocean productivity generally leads to high foraminiferal abundance due to high food availability (Schiebel and Hemleben, 2017; Tapia et al., 2022). Planktic foraminiferal abundance may coincide with the peak of fluorescence at a certain depth in the water column. Curiously, we do not observe any strong correlation between planktic foraminiferal abundance and productivity parameters such as sedimentary TOC and seawater fluorescence. This might have to do with the substantial scatter in the planktic foraminiferal abundance data. Another reason might be due to the inherent flaw of the approach in correlating the average fluorescence of the upper 0–400 m water column with foraminifera data, whereas the abundance of foraminifera likely follows the peak fluorescence at a certain depth that varies from site to site.

In the case of benthic foraminifera, the effect of ocean productivity (i.e., TOC) and bottom water oxygen content are highly complex and not always straightforward (Jorissen et al., 2007, 1995). Generally speaking, as surface ocean productivity increases, the flux of organic matter (food) to the seafloor tends to increase as well. Higher fluxes of organic matter to the seafloor may help benthic foraminifera to thrive; however, the decomposition of large amount of organic matter may lead to a depletion of the bottom water oxygen content due to the higher oxygen demand by more active remineralization. One effect of the oxygen depletion on benthic foraminifera is a shift in the size distribution toward the smaller size class (i.e., 63–125 µm) (Bernhard and Sen Gupta, 1999; Sen Gupta and Machain-Castillo, 1993), a condition that may affect our %P data as they are based on the foraminiferal abundances >125 µm. However, we posit that oxygen content is an unlikely driver of %P off Taiwan as the lowest oxygen value of the bottom water (~54.3 $\mu molL^{-1}$) in the study area is almost three times as high as the threshold (<22 μmL^{-1}) that is known to affect foraminiferal dynamics (Levin and Gage, 1998). The ecological response of benthic foraminifera to environmental parameters is highly complex, however our data show that bathymetry exert the strongest control on benthic foraminifera. This finding is in agreement with the concept that food (quantity and quality), the most relevant controlling factors of benthic foraminiferal ecology (Beck Eichler and Barker, 2020; Gooday, 2003; Jorissen et al., 2007, 1995; van der Zwaan et al., 1999) is somehow modulated by water depth. Overall, bathymetry still exerts the strongest control on the spatial distribution of %P despite minor influences from other hydrographic parameters.

4.3 %P-water depth relationship in different geological and sedimentological settings off Taiwan

In general, the %P off Taiwan increases exponentially with water depth ($R^2 = 0.72$; Fig. 4a). Notably, some data from the Southern Okinawa Trough, Hoping-Nanao-Hateruma Basins, and the Gaoping sector deviate strongly from the general trend (Fig. 4a and 4b).

The distribution of foraminiferal tests in the sediments is modulated by the interplay of the (1) production of foraminiferal test and sedimentation rate; (2) transport of foraminiferal test by ocean currents; (3) destruction (dissolution); (4) reworking of sediment and subsequent downslope transport and redeposition (Schmuker, 2000). Consequently, any index based on foraminiferal material will be susceptible to the above-mentioned processes. Indeed, previous studies have attributed the occurrence of “anomalously” low or high %P to downslope sediment transport (Hayward et al., 2019; Yamasaki and Miyako, 2010), or calcite dissolution in organic-rich sediments (in front of Mississippi River, Gulf of Mexico) (Parker, 1954). In the following three sub-sections, we discuss possible factors causing the anomalously low %P values in the Southern Okinawa Trough sector (section 4.3.1), Hoping-Nanao-Hateruma Basins (section 4.3.2), and submarine canyons in the Gaoping sector (section 4.3.3).

4.3.1 Low planktic foraminiferal abundance and downslope sediment transport in Southern Okinawa Trough

Overall, the %P distribution in the Southern Okinawa Trough is characterized by relatively low values (Fig. 3b and 3c) and substantial variability especially in the bathymetric range of ~1000–1500 m (Fig. 4b). Here, despite a moderate abundance of benthic foraminifera, the planktic foraminiferal abundance is the lowest among all the sectors assessed (Fig. 2a and 2b). Despite the lower-than-average planktic foraminiferal abundance, it is still twice as large as that of benthic foraminiferal abundance (compare the median values of gray boxplot in Fig. 2a and 2b). Therefore, the variability in %P here is likely driven by the variability in planktic foraminiferal abundance.

The abundance of planktic foraminiferal tests in sediments reflects the balance between the destruction and production of these calcite tests. Consequently, a low number of foraminiferal tests in surface sediments in the Southern Okinawa Trough might be the result of conditions that favor the destruction of the foraminiferal calcite tests. The preservation of carbonate in sediments varies as a function of the solubility of the carbonate in the seawater, with high (low) solubility favoring the destruction (preservation) of the foraminiferal calcite (Berger and Diester-Haass, 1988; Bostock et al., 2011). The depth where the solubility of the calcite changes is known as Calcite Saturation Horizon (CSH) (Bostock et al., 2011), and its position in the water column varies across basins as a function of the water pressure, in-situ temperature, and water chemistry. The modern Calcite Saturation Horizon in the Southern Okinawa Trough is located at ~1600 m water depth (GLODAP dataset, transect P03-W; Fig. 6a), close to the lower end of the bathymetric range characterized by large %P variability. Therefore, it is possible that the low number of foraminiferal tests in this sector reflects a relatively shallow position of the CSH causing calcite dissolution. However, the abundance of planktic foraminifera below (1600 – 1800 m) and above (1400 – 1600 m) the CSH show no significant change (Fig. 6a), arguing against calcite dissolution as the main driver of the low presence of planktic foraminiferal tests in the sediment.

The production of planktic foraminiferal tests in the water column is generally related to water fertility (Schiebel and Hemleben, 2017; Tapia et al., 2022). Consequently, the oligotrophic Kuroshio Current flowing northward along the eastern coast of Taiwan (Liang et al., 2003) may reduce the planktic foraminiferal abundances and, in turn, the %P in Southern Okinawa Trough. However, relatively high planktic foraminiferal abundances and %P values occur at some sites within the Southern Okinawa Trough (Fig. 3c) and at sites located offshore the eastern flank off Taiwan along the path of Kuroshio Current (i.e., Taitung-Hualien and in Hoping-Nanao-Hateruma Basins) (Fig. 3b). Moreover, the Southern Okinawa Trough is influenced by topographically steered upwelling centers that further fertilize the upper ocean, increasing its fertility (Jan et al., 2011; Lee et al., 2004). Altogether these findings suggest that lower ocean fertility due to Kuroshio Current is not the main driver of the low and variable %P values in this basin.

>> Figure 6 <<

The amount of exported carbon to the seafloor generally reflects the marine productivity in the euphotic zone. Therefore, the organic carbon content in surface sediments may shed light on the relationship between marine productivity and %P. Interestingly, the TOC content in the sediments from the Southern Okinawa Trough is slightly higher than the rest of the dataset. If the aforementioned positive relationship between marine productivity and %P applies to this region, high TOC content in Southern Okinawa Trough sediment argues against low water fertility as the main reason for the low planktic foraminiferal content in the sediments. Typically, the TOC content in marine sediments shows a seaward decrease with more OC-rich sediments close to land due to terrigenous input. This trend is broadly true for sediments off Taiwan except in the Southern Okinawa Trough (Fig. 5d), where the TOC content further away from land (>1000 m water depth) is higher than the TOC content on the adjacent shelf and the mouth of the Lanyang River (Fig. 5f, g). Previous studies have explained this pattern as a consequence of the overprint of the riverine export, as the low TOC values near river mouth reflect a strong mineral dilution effect, a distinctive characteristic of mountainous watersheds off Taiwan (Jeng et al., 2003; Kao and Liu, 1996; Kao et al., 2003). Indeed, studies based on organic composition have suggested that riverine materials from the Lanyang River are not the main source of organic components in the sediments of the Southern Okinawa Trough Taiwan (Jeng et al., 2003; Kao and Liu, 1996; Kao et al., 2003), since the δ^{13}Corg and δ^{15}N values observed here overlap with those from the inner shelf of East China Sea. Similarly, several studies based on clay mineral and detrital composition of sediments in the Southern Okinawa Trough agree on an inner shelf-Southern Okinawa Trough sediment flux route (Chen et al., 2017; Chung et al., 2003; Kao et al., 2003; Lee et al., 2004). The topographic constraint of the Kuroshio Current against the East China Sea leads to a southwest flow and the formation of 100 km cyclonic eddies centered on the Mien-Hua Canyon (Chen et al., 2017; Chiang et al., 2022; Chung et al., 2003; Kao et al., 2003; Lee et al., 2004). These eddies promote the retention and resuspension of suspended particles on the slope of the East China Sea shelf. From here, the sediments are transported downslope by gravity flows to the deeper parts of the Southern Okinawa Trough (Chen et al., 2017; Chiang et al., 2022; Chung et al., 2003; Kao et al., 2003; Lee et al., 2004). The interplay of water column dynamics, lateral transport and retention/resuspension of sediments makes the Southern Okinawa Trough one of the highest particle flux regimes in the world, with sedimentation rates ranging from <0.01 – 0.08 g cm yr^{-1} in the northern–central part to ~0.1 – 0.95 g cm yr^{-1} in the southern part (Huh et al., 2006, 2004; Lee et al., 2004; Su and Huh, 2002).

Previous studies in the Southern Okinawa Trough using sedimentary ^{210}Pb concluded that in addition to hemipelagic sedimentation, gravity flows (i.e., turbidity flow) are the main source of sedimentary material here sedimentary transport processes (Huh et al., 2006, 2004). Huh et al (2006) noted that 1) the sites located on the slope had a lower ^{210}Pb mass accumulation rates relative to sites at the same water depths further offshore Taiwan and 2) that a depression at the base of the slope below the 1400 m isobath in the western part of the Southern Okinawa Trough between 122.3 and 122.7 ºE was characterized by extremely high sedimentation rates (0.4 – ~1.5 cm yr^{-1}). The authors interpreted this pattern as the result of the transport of sedimentary material from the slope toward the basin floors via episodic inputs of turbidites triggered by earthquakes, which then led to the formation of a zone of ~300 km^2 of "abnormally" high sediment input (Huh et al., 2006, 2004; Lee et al., 2004). Interestingly, the lowest %P values observed in the Southern Okinawa Trough (Fig. 7a) occur within this zone. The grid 25–24.75 ºN and 122.3–122.7 ºE is characterized by sedimentation rates >1 cm y^{-1} (Fig. 7a). The sites in this grid cover a relatively small bathymetric range between ~1000 – ~1500 m water depth, but %P values vary substantially between 25% to 80% (Fig. 4b). Given the bathymetric range, the expected %P values as observed in other regions should be in the range of 85% and 94%, but values as low as 25% that is typical for shallow shelf can be observed in the Southern Okinawa Trough (Fig. 4a). In line with previous studies, gravity flows triggered by earthquakes may be a mechanism via which sediments from the shelf and slope can be transported to the deeper part of the basin. As sediments from the shelf typically contain low planktic foraminiferal content and low %P value, the presence of these sediments in the deep basin would thus lead to lower values in %P and planktic foraminiferal abundance, as observed in the Southern Okinawa Trough. The occurrence of gravitationally displaced individuals e.g., shallow water genera such as *Amphistegina*, *Calcarina*, *Neorotalia*, *Elphidium* (Fig. S2) in the surface sediments of some stations located below ~1000 m water depth (stations OR1-642-BC22; OR1-0715-22) also argue in favor of the supply of sediments from shallower depths via gravity flows. Taken together, we argue that the low concentration of planktic foraminifera in the Southern Okinawa Trough surface sediments (Fig. 2b) may have been a result of the dilution of the locally produced biogenic material by detrital material transported by gravity flows.

>> Figure 7 <<

4.3.2 Possible bias by carbonate dissolution on %P values in Hoping-Nanao-Hateruma Basins

The %P values of sediments from the Hoping-Nanao-Hateruma Basins are amongst the highest off Taiwan (Fig. 4a), despite the relatively low planktic foraminiferal abundance here compared to other pelagic regions with bathymetry > 2000 m such as Hengchun Ridge (Fig. 2b).

Nevertheless, the planktic foraminiferal abundance in these basins are >20 times higher the benthic foraminiferal abundance (see sections 3.2 and 3.3; Fig. 2), thus exerts a stronger influence on the %P values than does its benthic counterpart. Notably, in contrast to the general positive relationship with bathymetry (Fig. 2d), planktic foraminiferal abundance in Hoping-Nanao-Hateruma Basins decreases with increasing water depth (Fig. 6b), with the largest variability occurring within the Carbonate Saturation Horizon located at ~3000 m. The aforementioned relationship between planktic foraminiferal abundance and water depth plus the fact that the average water depth in this region is ~3500 m both indicate that carbonate dissolution maybe an issue here.

The %P values in Hoping-Nanao-Hateruma Basins are within a small range between ~86 and 99.8 % except for the site MD18-3531BC (water depth of 3590 m) where the %P = ~51%; (Fig. 4a). We do not have %P value for deeper sites because the foraminiferal counts here do not pass the threshold of at least 50 counts. Site MD18-3531BC is characterized by planktic foraminiferal abundance (3.7 ind. g^{-1}) (see Table S1) several times below the average of this region (~23 ind. g^{-1}; Fig. 2a). The site is located below the Carbonate Saturation Horizon where carbonate dissolution is extensive. The tests of planktic foraminifera are more susceptible to dissolution than those of benthic foraminifera (Corliss and Honjo, 1981; Regenberg et al., 2013), thus it is plausible that the low %P value (~51%; Fig. 4a) at site MD18-3531BC reflects the preferential loss of planktic foraminiferal tests due to carbonate dissolution. Interestingly, the %P values at the other two sites in the Hateruma Basin (MD18-3529BC and MD18-3530BC; %P >89) are much higher than that at MD18-3531BC (Fig. 8). These sites are ~100–200 m shallower than site MD18-3531BC but still below the Carbonate Saturation Horizon, thus should be equally susceptible to carbonate dissolution. The sites in the Hateruma Basin are also marked by large variability in planktic foraminiferal abundance, ranging from 3.7 ind. g^{-1} to 72 ind. g^{-1} (Fig. 8). Given the proximity of the sites (see Fig. 1) and thus similarity in hydrography, it seems unlikely that this variability stems from large changes in the fluxes of planktic foraminifera.

Instead, we hypothesize that the variability in planktic foraminiferal numbers in the rather small Hateruma Basin may reflect downslope transport of sediment from relatively deep localities (>1000 m) where the %P value is similar to that in the autochthonous sediments. This scenario is partially supported by the grain size distribution in the Hoping-Nanao-Hateruma Basins. Here, several studies have used grain size changes to identify turbidites from sediment of hemipelagic origin (Dezileau et al., 2016; Lehu et al., 2015; Nayak et al., 2021). Turbidites typically appear as departures from fine sediments (hemipelagic <10 μm) (Lehu et al., 2015) toward coarser sizes. The surface sediment of the core MD18-3531BC show the highest percentage of sand (>63 μm) among the sites in the Hateruma Basin (Fig. 8), suggesting a possible turbidite origin of the sediment.

The complex interplay between carbonate dissolution and downslope transport that is highly variable in space therefore alters the relationship between %P and bathymetry in the sites in Hoping-Nanao-Hateruma Basins. Allochthonous sediments especially those from a much shallower depth may alter the proportion of planktic and benthic foraminiferal tests in the sediments, while dissolution preferentially removes planktic foraminiferal tests from the sediment; both scenarios lead to lower %P values. A qualitative estimation of the dominant factor on the %P (depth v. dissolution v. downslope transport) might be possible by considering additional information such as grain size distribution, total abundances of planktic foraminifera, fragmentation, and foraminiferal fauna.

>> Figure 8 <<

4.3.3 Low foraminiferal abundance and %P values in submarine canyons off Southwestern Taiwan

The sediments located in submarine canyons (Gaoping and Fangliao; see Fig. 1d) are characterized by particularly low abundances of planktic and benthic foraminifera, compared to other samples collected from the Gaoping sector (Fig. S3). As this low abundance only occurs within the canyons it is unlikely to be caused by processes involving large spatial coverage i.e., production and preservation (dissolution). Instead, smaller scale processes associated with the canyon dynamics are more likely to be responsible for the low foraminiferal abundance.

The Gaoping River provides 23 to 49 Mt yr^{-1} of terrestrial material to the Gaoping Submarine Canyon (Huh et al., 2009; Lee et al., 2015). If deposited in the canyon, such a large amount of terrestrial material may in principle dilute the biogenic component of marine origin in the sediment. Riverine runoff is heavily influenced by regional climatic patterns. For instance, typhoons can exert a strong effect on the delivery of material to the canyon as the heavy rains on the upstream catchment area increase the flow rate of the Gaoping River as well as its sediment load (Lee et al., 2015; Liu et al., 2009, 2006). As a typhoon approaches, events of sediment-flushing down-canyon (as gravity flow) occurs (Chung et al., 2009; Huh et al., 2009; Lee et al., 2009b, 2009a; Liu et al., 2009, 2006; Su et al., 2012). Su et al (2012) highlighted the high energy associated with these gravity flows events as they were the most likely culprit of the submarine cable breakage at the landfall of the typhoon Morakot between 7 to 9 of August (2009). Due to this process, only 20% of the riverine sediment load from Gaoping River is retained in the canyon, the rest of it being delivered to the deep basin (Huh et al., 2009). The constant flushing of sediment also leads to relatively low sedimentation rates in the canyon relative to the neighboring shelf (Hu et al., 2009; Fig 7b). Therefore, it is plausible that gravity flows may remove foraminiferal tests from the sediments in the uppermost parts of the canyon and transport them downslope. As the kinetic energy of the gravity flow dissipates some foraminiferal test may be released and re-deposited at different parts of the canyon. These processes might lead to low foraminiferal abundance in the canyons.

Typhoons also result in cross-shelf transport. For instance, benthic foraminifera have been found in a set of sediment traps moored off the Gaoping River during the landfall of the typhoon Kay-tak (2000) (Lin et al., 2005). The isotopic compositions of the benthic foraminifera recovered from the upper (186 m) and lower (236 m) traps suggest calcification depth <50 m, thus they must have been transported from shallower localities. This finding highlights a connection between typhoon occurrence and cross-shelf transport of foraminiferal tests, which may transport low %P sediments (due to higher abundance of benthic foraminifera) from the shallow shelf to the deep canyon and the mixing of sediments will thus lower the %P value in the canyon. Foraminiferal abundance at most sites in the Gaoping and Fangliao submarine canyons is too low for %P calculation. The only three canyon sites containing enough foraminiferal tests (n>50) for the %P calculation, namely OR3-1367-G4 (436 m), OR3-1963-C59 (677 m) (Gaoping Submarine Canyon), and OR1-1188-FL1 (570 m) (Fangliao Canyon), show low %P values for the bathymetric range (Fig. 3d, 4a and S2c) albeit still within the 95% prediction range (Fig. 4a). These low %P values might be a result of the aforementioned cross-shelf transport. It is possible that this type of transport may in part leads to the relatively large scatter in foraminiferal abundance and %P value in the Gaoping sector (Fig. 4a).

On the other hand, high %P (60-95%) values are observed for four sites on the shallow shelf off Southwestern Taiwan at the entrance of the Taiwan Strait, namely OR3-1367-C4 (54 m); OR3-1420-C8 (107); OR3-1367-C45 (133 m), and C49 (169 m) (Fig. 3d). Since the intrusion of the Kuroshio Branch Current and South China Sea Current feed the Taiwan Current that flows across the Taiwan Strait (Fig.1b), the high %P values may be caused by the lateral advection of planktic foraminifera produced further south where the water column is deeper and then deposited on the shallow shelf typically characterized by low abundance of planktic foraminifera (Fig. 2b). In fact, laterally transported planktic foraminifera by East Auckland Current has also been invoked to explain high %P values in the shelf sediments off New Zealand Northland (Hayward et al., 2010).

4.4 Regional and global regression function of %P–water depth

%P values in marine sediments off Taiwan generally vary with bathymetry (section 4.3) but may be strongly influenced by downslope or cross-shelf sediment transport (section 4.3.1, 4.3.2, 4.3.3), lateral transport of planktic foraminifera (section 4.3.3) and carbonate preservation issues (section 4.3.2). Data affected by these processes (i.e. data points lying outside the 95% prediction bound in Fig. 4a) deviate from the general %P–water depth relationship (Fig. 4a). Therefore, these biased data are omitted from the regression analysis to obtain the “true” %P–bathymetry relationship in autochthonous sediments off Taiwan (n = 81; Fig. 9). The exponential regression function is as follows:

Water depth (m) = 27.472*exp(0.04245*%P)

where a value of %P = 100 would result in a depth estimate of 1916 m, whereas %P = 1 would yield 27 m. In other words, when used to reconstruct bathymetry, this equation will not yield any estimate that is >1916 m; for instance, all the water depth estimates for samples in the Hoping-

Nanao-Hateruma Basins are too shallow by ~1500 m (Fig. 9c). Despite a strong correlation indicated by the coefficient of determination (R^2= 0.72), it is clear from the residuals that the water depth estimates may be overestimated or underestimated by ~2000 m (Fig. 9c), with a mean (absolute residual) of ~530 m. Due to its exponential relationship, the regression is more sensitive within the depth range of ~200 and ~1000 m. It also yields more accurate water depth estimates for shallow regions <500 m, e.g. at Changyun Sand Ridge (mean absolute residual = 5 m) and Gaoping sector (mean absolute residual = 434 m). Therefore, although this exponential regression may be useful as a qualitative tool to reconstruct paleobathymetry off Taiwan, care should be exercised when interpreting the water depth estimates obtained as they may not be interpreted quantitatively, especially at the high end of the %P range.

The visual comparison of several regional %P-depth datasets (Fig 9a) indicates minor regional differences as the slope and intercept of the equations differ, but all regressions agree within uncertainty (95% confidence interval). Notably, the regression off Taiwan shows a striking similarity with that from the Gulf of Mexico which is under the influence of the Mississippi River. Combining the regional datasets yields a global calibration (n = 827) with a R^2 value of 0.85 (Fig 9b). The global regression line is almost identical to the Taiwan regression line but with an improved correlation likely due to the much larger dataset. When applied to the Taiwan dataset the global calibration yields comparable residuals (mean = 805 m compared to 530 m from the Taiwan calibration) as those obtained from the Taiwan calibration. This suggests that the %P-depth relationship off Taiwan is similar to the global relationship, but a local calibration would perform better in the reconstruction of water depth despite its slightly lower R^2 value.

>> Figure 9<<

4.5 %P as a tool for the reconstruction of paleobathymetry, paleogeohazard and paleoceanography

Despite the aforementioned uncertainties (section 4.4), the Taiwan %P-depth calibration reported here represents the first of its kind for paleobathymetric reconstructions in this region. The application of this modern analog-based calibration might help to generate at least semiquantitative bathymetry estimates, which can be used to reveal the depositional setting of the many outcrops in Taiwan and to shed more light on processes such as the rapid uplift of the central range of Taiwan since the Plio-Pleistocene (i.e., Lai et al., 2022). Further effort should be directed to refine the calibration model by increasing the sample size, including diversity indices and stressor species of benthic foraminifera in the %P calculation, and/or including the census counts of smaller size fractions (i.e., 63–125 µm).

Our results also demonstrate that %P responds to alterations in the sedimentation process (i.e., downslope transport), manifesting as outliers in the %P-water depth relationship. Off Taiwan, in the sectors of Gaoping and Southern Okinawa Trough, the sites with lower than expected %P values can be explained by the downslope transport of sediment, triggered by typhoons or earthquakes. At deep sites located below the Carbonate Saturation Horizon e.g. in Hoping-Nanao-Hateruma Basins, carbonate dissolution may also lead to low %P values as planktic foraminiferal tests are preferentially dissolved compared to their more robust benthic counterparts (section 4.3.2). For these deep sites, we suggest that additional data such as grain size and abundance of foraminiferal tests and diversity indices to be used in tandem to improve the robustness of the %P. The fact that %P traces downslope sediment transport and lateral transport in the water column (section 4.3.2) also means that it has the potential to flag sites and sediment sequences that are unsuitable for paleoceanographic studies that rely on locally produced biogenic material. Therefore, applying %P downcore allows the reconstruction of past occurrences of gravity flow as well as assessing the sedimentary depth horizons that are suitable for paleoceanographic studies, thereby providing clues on possible links between gravity flows and climate variability.

5. CONCLUSIONS

The spatial patterns of planktic and benthic foraminifera test in >100 surface sediment samples off Taiwan were determined and compared with hydrographic and bulk sedimentary parameters (grain size distribution and TOC content). These data were used to assess the potential of %P as a tool to detect downslope sediment transport and reconstruct paleobathymetry.

The following are specific conclusions based on the results:

- The abundance of planktic foraminifera increases with water depth while the opposite is true for the abundance of benthic foraminifera.
- The %P-water depth relationship based on counts with >50 and >100 tests are comparable, suggesting that at least for this dataset the threshold of >50 foraminifera count is reasonable.
- Of all the hydrographic and environmental parameters, %P shows the strongest correlation with water depth. %P-water depth relationship in marine sediments off Taiwan shows the same first-order pattern as in other regions and is similar to the global calibration.
- The %P values of surface sediments in Southern Okinawa Trough, Gaoping Submarine Canyon and Hoping-Nanao-Hateruma Basins are relatively low compared to those from a similar bathymetric range.
  - The low %P values in the Southern Okinawa Trough seem to reflect dilution effect due to the arrival of fine material from the East China Shelf area and material transported downslope by gravity flows toward the base of the basin.
  - Low foraminiferal abundances and %P values in Gaoping Submarine Canyon area are likely a result of cross-shelf and downslope sediment transport.
  - In the Hoping-Nanao-Hateruma Basins the %P seems to reflect the interplay between downslope transport of sediment and carbonate dissolution.
- The relationship %P-water calculated (water depth (m) = 27.472*exp(0.042451*%P)) may be useful for deducing paleobathymetry in the range of ~30 to ~2000 m water depth off Taiwan.
- %P has the potential to capture alterations in the sedimentation process, therefore its application downcore might help to identify both the occurrence of downslope transport and sequences that are suitable for paleoceanographic reconstruction.

6. Author's contribution

RT, SLH and CCS designed and conceptualized the study. CCS, HLL, KTJ, YPC, ITL, SLH provided surface sediment samples as well as unpublished bulk and grain size data. SCL and RT prepared and analyzed the sediment samples for foraminifera. SCL prepared and analyzed bulk and grain size analysis as well as requested hydrographic data. Data analysis was performed by SCL and RT. Initial draft in the form of a MSc thesis excluding data from the EAGER samples was written by SCL with help from SLH. The final manuscript was written by RT and SLH with the contribution from all co-authors who approved its final version.

7. Acknowledgments

This study was funded by Ministry of Science and Technology (MOST) R.O.C. through grants 108-2116-M-002-008, 109-2116-M-002-014 and 110-2116-M-002-007. SLH acknowledges grant 107-2611-M-002-021-MY3. We thank the crew and scientists participating in OR1, OR2, OR3, NOR1 and EAGER cruises. Technical support and laboratory assistance from Shen-Ting Hsu (IONTU) are highly appreciated.

8. Data Availability Statement

Data generated in this study will be available upon request to the main author until their online publication on PANGAEA database (www.pangaea.de).

9. References

Ash-Mor, A., Bookman, R., Kanari, M., Ben-Avraham, Z., Almogi-Labin, A., 2017. Micropaleontological and taphonomic characteristics of mass transport deposits in the northern Gulf of Eilat/Aqaba, Red Sea. Mar. Geol. 391, 36–47. doi:10.1016/j.margeo.2017.07.009

Ash-Mor, A., Almogi-Labin, A., Bouchet, V.M.P., Seuront, L., Guy-Haim, T., Ben-Avraham, Z., Bookman, R., 2021. Going with the flow: Experimental simulation of sediment transport from a foraminifera perspective. Sedimentology. doi:10.1111/sed.12945

Beck Eichler, P.P., Barker, C.P., 2020. Benthic foraminiferal ecology: indicators of environmental impacts. Springer International Publishing, Cham. doi:10.1007/978-3-030-61463-8

Berger, W.H., Diester-Haass, L., 1988. Paleoproductivity: The benthic/planktonic ratio in foraminifera as a productivity index. Mar. Geol. 81, 15–25. doi:10.1016/0025-3227(88)90014-X

Bernhard, J.M., Sen Gupta, B.K., 1999. Foraminifera of oxygen-depleted environments, in: Modern Foraminifera. Springer Netherlands, Dordrecht, pp. 201–216. doi:10.1007/0-306-48104-9_12

Bostock, H.C., Hayward, B.W., Neil, H.L., Currie, K.I., Dunbar, G.B., 2011. Deep-water carbonate concentrations in the southwest Pacific. Deep Sea Research Part I: Oceanographic Research Papers 58, 72–85. doi:10.1016/j.dsr.2010.11.010

Chen, C., Lin, H.-L., 2017. Applying Benthic Foraminiferal Assemblage to Evaluate the Coral Reef Condition in Dongsha Atoll lagoon. Zool. Stud. 56, e20. doi:10.6620/ZS.2017.56-20

Chen, C.-T.A., Kandasamy, S., Chang, Y.-P., Bai, Y., He, X., Lu, J.-T., Gao, X., 2017. Geochemical evidence of the indirect pathway of terrestrial particulate material transport to the Okinawa Trough. Quaternary International 441, 51–61. doi:10.1016/j.quaint.2016.08.006

Chiang, C.-S., Yu, H.-S., Noda, A., TuZino, T., 2022. The huapinghsu channel/mienhua canyon system as a sediment conduit transporting sediments from offshore north taiwan to the southern okinawa trough. Front. Earth Sci. 9. doi:10.3389/feart.2021.792595

Chien, F.-C., Kuo, H.-C., 2011. On the extreme rainfall of Typhoon Morakot (2009). J. Geophys. Res. 116. doi:10.1029/2010JD015092

Chung, C.-H., You, C.-F., Chu, H.-Y., 2009. Weathering sources in the Gaoping (Kaoping) river catchments, southwestern Taiwan: Insights from major elements, Sr isotopes, and rare earth elements. Journal of Marine Systems 76, 433–443. doi:10.1016/j.jmarsys.2007.09.013

Chung, Y., Chung, K., Chang, H.C., Wang, L.W., Yu, C.M., Hung, G.W., 2003. Variabilities of particulate flux and 210Pb in the southern East China Sea and western South Okinawa Trough. Deep Sea Res. Part II Top. Stud. Oceanogr 50, 1163–1178. doi:10.1016/S0967-0645(03)00016-X

Corliss, B.H., Honjo, S., 1981. Dissolution of Deep-Sea Benthonic Foraminifera. Micropaleontology 27, 356. doi:10.2307/1485191

Dezileau, L., Lehu, R., Lallemand, S., Hsu, S.K., Babonneau, N., Ratzov, G., Lin, A.T., Dominguez, S., 2016. Historical Reconstruction of Submarine Earthquakes Using^{210} Pb,^{137} Cs, and^{241} Am Turbidite Chronology and Radiocarbon Reservoir Age Estimation off East Taiwan. Radiocarbon 58, 25–36. doi:10.1017/RDC.2015.3

Gibson, T.G., 1989. Planktonic benthonic foraminiferal ratios: Modern patterns and Tertiary applicability. Mar. Micropaleontol. 15, 29–52. doi:10.1016/0377-8398(89)90003-0

Gooday, A.J., 2003. Benthic foraminifera (Protista) as tools in deep-water palaeoceanography: environmental influences on faunal characteristics. Adv. Mar. Biol. 46, 1–90. doi:10.1016/s0065-2881(03)46002-1

Hammer, Ø., Harper, D., Ryan, P., 2001. PAST: PALEONTOLOGICAL STATISTICS SOFTWARE PACKAGE FOR EDUCATION AND DATA ANALYSIS. Palaeontologia electronica (Online) 4, 9.

Hayward, B.W., Grenfell, H.R., Sabaa, A.T., Neil, H., Buzas, M.A., 2010. Recent New Zealand deep- water benthic foraminifera: taxonomy, ecologic distribution, biogeography, and use in paleoenvironmental assessment.

Hayward, B.W., Sabaa, A.T., Triggs, C.M., 2019. Using foraminiferal test-size distribution and other methods to recognise Quaternary bathyal turbidites and taphonomically-modified faunas. Mar. Micropaleontol. 148, 65–77. doi:10.1016/j.marmicro.2019.03.008

Hayward, B.W., Triggs, C.M., 2016. Using multi-foraminiferal-proxies to resolve the paleogeographic history of a lower miocene, subduction-related, sedimentary basin (waitemata basin, new zealand). Journal of Foraminiferal Research 46, 285–313. doi:10.2113/gsjfr.46.3.285

Huang, T.-H., Chen, C.-T.A., Zhang, W.-Z., Zhuang, X.-F., 2015. Varying intensity of Kuroshio intrusion into Southeast Taiwan Strait during ENSO events. Continental Shelf Research 103, 79–87. doi:10.1016/j.csr.2015.04.021

Huh, C.-A., Lin, H.-L., Lin, S., Huang, Y.-W., 2009. Modern accumulation rates and a budget of sediment off the Gaoping (Kaoping) River, SW Taiwan: A tidal and flood dominated depositional environment around a submarine canyon. Journal of Marine Systems 76, 405–416. doi:10.1016/j.jmarsys.2007.07.009

Huh, C.-A., Su, C.-C., Liang, W.-T., Ling, C.-Y., 2004. Linkages between turbidites in the southern Okinawa Trough and submarine earthquakes. Geophys. Res. Lett. 31. doi:10.1029/2004GL019731

Huh, C.-A., Su, C.-C., Wang, C.-H., Lee, S.-Y., Lin, I.-T., 2006. Sedimentation in the Southern Okinawa Trough — Rates, turbidites and a sediment budget. Mar. Geol. 231, 129–139. doi:10.1016/j.margeo.2006.05.009

Jan, S., Chen, C.-C., Tsai, Y.-L., Yang, Y.J., Wang, J., Chern, C.-S., Gawarkiewicz, G., Lien, R.-C., Centurioni, L., Kuo, J.-Y., 2011. Mean structure and variability of the cold dome northeast of taiwan. oceanog. 24, 100–109. doi:10.5670/oceanog.2011.98

Jeng, W.-L., Lin, S., Kao, S.-J., 2003. Distribution of terrigenous lipids in marine sediments off northeastern Taiwan. Deep Sea Res. Part II Top. Stud. Oceanogr 50, 1179–1201. doi:10.1016/S0967-0645(03)00017-1

Jones, R.W., 2013. Foraminifera and their Applications. Cambridge University Press, Cambridge. doi:10.1017/CBO9781139567619

Jorissen, F.J., de Stigter, H.C., Widmark, J.G.V., 1995. A conceptual model explaining benthic foraminiferal microhabitats. Mar. Micropaleontol. 26, 3–15. doi:10.1016/0377-8398(95)00047-X

Jorissen, F.J., Fontanier, C., Thomas, E., 2007. Chapter Seven Paleoceanographical Proxies Based on Deep-Sea Benthic Foraminiferal Assemblage Characteristics, in: Proxies in Late Cenozoic Paleoceanography, Developments in Marine Geology. Elsevier, pp. 263–325. doi:10.1016/S1572-5480(07)01012-3

Kao, S.-J., Liu, K.-K., 1996. Particulate organic carbon export from a subtropical mountainous river (Lanyang Hsi) in Taiwan. Limnol. Oceanogr. 41, 1749–1757. doi:10.4319/lo.1996.41.8.1749

Kao, S.J., Lin, F.J., Liu, K.K., 2003. Organic carbon and nitrogen contents and their isotopic compositions in surficial sediments from the East China Sea shelf and the southern Okinawa

Trough. Deep Sea Res. Part II Top. Stud. Oceanogr 50, 1203–1217. doi:10.1016/S0967-0645(03)00018-3

Lai, L.S.-H., Dorsey, R.J., Horng, C.-S., Chi, W.-R., Shea, K.-S., Yen, J.-Y., 2022. Extremely rapid up-and-down motions of island arc crust during arc-continent collision. Commun. Earth Environ. 3, 100. doi:10.1038/s43247-022-00429-2

Lee, I.-H., Lien, R.-C., Liu, J.T., Chuang, W., 2009a. Turbulent mixing and internal tides in Gaoping (Kaoping) Submarine Canyon, Taiwan. Journal of Marine Systems 76, 383–396. doi:10.1016/j.jmarsys.2007.08.005

Lee, I.-H., Wang, Y.-H., Liu, J.T., Chuang, W.-S., Xu, J., 2009b. Internal tidal currents in the Gaoping (Kaoping) Submarine Canyon. Journal of Marine Systems 76, 397–404. doi:10.1016/j.jmarsys.2007.12.011

Lee, S.-Y., Huh, C.-A., Su, C.-C., You, C.-F., 2004. Sedimentation in the Southern Okinawa Trough: enhanced particle scavenging and teleconnection between the Equatorial Pacific and western Pacific margins. Deep Sea Research Part I: Oceanographic Research Papers 51, 1769–1780. doi:10.1016/j.dsr.2004.07.008

Lee, T.-Y., Huang, J.-C., Lee, J.-Y., Jien, S.-H., Zehetner, F., Kao, S.-J., 2015. Magnified Sediment Export of Small Mountainous Rivers in Taiwan: Chain Reactions from Increased Rainfall Intensity under Global Warming. PLoS ONE 10, e0138283. doi:10.1371/journal.pone.0138283

Lehu, R., Lallemand, S., Hsu, S.-K., Babonneau, N., Ratzov, G., Lin, A.T., Dezileau, L., 2015. Deep-sea sedimentation offshore eastern Taiwan: Facies and processes characterization. Mar. Geol. 369, 1–18. doi:10.1016/j.margeo.2015.05.013

Levin, L.A., Gage, J.D., 1998. Relationship between oxygen, organic matter and the diversity of bathyal macrofauna. Deep Sea Research Part II 45, 129–163.

Liang, W.D., Tang, T.Y., Yang, Y.J., Ko, M.T., Chuang, W.S., 2003. Upper-ocean currents around Taiwan. Deep Sea Res. Part II Top. Stud. Oceanogr 50, 1085–1105. doi:10.1016/S0967-0645(03)00011-0

Lin, H.-L., Hsieh, H.-Y., 2007. Seasonal variations of modern planktonic foraminifera in the South China Sea. Deep Sea Res. Part II Top. Stud. Oceanogr 54, 1634–1644. doi:10.1016/j.dsr2.2007.05.007

Lin, H.-L., Liu, J.T., Hung, G.-W., 2005. Foraminiferal shells in sediment traps: Implications of biogenic particle transport in the Kao-ping submarine canyon, Taiwan. Continental Shelf Research 25, 2261–2272. doi:10.1016/j.csr.2005.09.001

Lin, H.-L., Sheu, D.D.-D., Yang, Y., Chou, W.-C., Hung, G.-W., 2011. Stable isotopes in modern planktonic foraminifera: Sediment trap and plankton tow results from the South China Sea. Mar. Micropaleontol. 79, 15–23. doi:10.1016/j.marmicro.2010.12.002

Lin, H.-L., 2014. The seasonal succession of modern planktonic foraminifera: Sediment traps observations from southwest Taiwan waters. Continental Shelf Research 84, 13–22. doi:10.1016/j.csr.2014.04.020

Liu, J.T., Hung, J.-J., Lin, H.-L., Huh, C.-A., Lee, C.-L., Hsu, R.T., Huang, Y.-W., Chu, J.C., 2009. From suspended particles to strata: The fate of terrestrial substances in the Gaoping (Kaoping) submarine canyon. Journal of Marine Systems 76, 417–432. doi:10.1016/j.jmarsys.2008.01.010

Liu, J.T., Lin, H.-L., Hung, J.-J., 2006. A submarine canyon conduit under typhoon conditions off Southern Taiwan. Deep Sea Research Part I: Oceanographic Research Papers 53, 223–240. doi:10.1016/j.dsr.2005.09.012

Ministry of Science and Technology – Republic of China, 2022. ODB – MOST [WWW Document]. Ocean Data Bank (ODB). URL https://www.odb.ntu.edu.tw/ (accessed 4.20.22).

Nayak, K., Lin, A.T.-S., Huang, K.-F., Liu, Z., Babonneau, N., Ratzov, G., Pillutla, R.K., Das, P., Hsu, S.-K., 2021. Clay-mineral distribution in recent deep-sea sediments around Taiwan: Implications for sediment dispersal processes. Tectonophysics 814, 228974. doi:10.1016/j.tecto.2021.228974

Nigam, R., Henriques, P.J., 1992. Planktonic percentage of foraminiferal fauna in surface sediments of the Arabian Sea (Indian Ocean) and a regional model for paleodepth determination. Palaeogeography, Palaeoclimatology, Palaeoecology 91, 89–98. doi:10.1016/0031-0182(92)90034-3

Olsen, A., Lange, N., Key, R.M., Tanhua, T., Álvarez, M., Becker, S., Bittig, H.C., Carter, B.R., Cotrim da Cunha, L., Feely, R.A., van Heuven, S., Hoppema, M., Ishii, M., Jeansson, E., Jones, S.D., Jutterström, S., Karlsen, M.K., Kozyr, A., Lauvset, S.K., Lo Monaco, C., Wanninkhof, R., 2019. GLODAPv2.2019 – an update of GLODAPv2. Earth Syst. Sci. Data 11, 1437–1461. doi:10.5194/essd-11-1437-2019

Parker, F.L., 1954. Distribution of the Foraminifera in the northeastern Gulf of Mexico. Bulletin of the Museum of Comparative Zoology at Harvard College. 111, 451–588.

Poppe, L.J., Eliason, A.H., Fredericks, J.J., Rendigs, R.R., Blackwood, R.D., Polloni, C.F., 2000. Grain size analysis of marine sediments: methodology and data processing., in: USGS East-Coast Sediment Analysis: Procedures, Database, and Georeferenced Displays. US Geological Survey Open-File Report,00-358 (CD-ROM). United States Geological Survey.

Regenberg, M., Schroder, J.F., Jonas, A.S., Woop, C., Gorski, L., 2013. Weight loss and elimination of planktonic foraminiferal tests in a dissolution experiment. Journal of Foraminiferal Research 43, 406–414. doi:10.2113/gsjfr.43.4.406

Schiebel, R., Hemleben, C., 2017. Planktic foraminifers in the modern ocean, 2d ed. Springer Berlin Heidelberg, Berlin, Heidelberg. doi:10.1007/978-3-662-50297-6

Schlitzer, R., 2002. Interactive analysis and visualization of geoscience data with Ocean Data View. Comput. Geosci. 28, 1211–1218. doi:10.1016/S0098-3004(02)00040-7

Schmuker, B., 2000. The influence of shelf vicinity on the distribution of planktic foraminifera south of Puerto Rico. Mar. Geol. 166, 125–143. doi:10.1016/S0025-3227(00)00014-1

Schröder-Adams, C.J., Boyd, R., Ruming, K., Sandstrom, M., 2008. Influence of sediment transport dynamics and ocean floor morphology on benthic foraminifera, offshore Fraser Island, Australia. Mar. Geol. 254, 47–61. doi:10.1016/j.margeo.2008.05.002

Schröeder, C.J., Scott, D.B., Medioli, F.S., 1987. Can smaller benthic foraminifera be ignored in paleoenvironmental analyses? Journal of Foraminiferal Research 17, 101–105. doi:10.2113/gsjfr.17.2.101

Seismological Center – Republic of China, 2022. Central Weather Bureau - Seismological Center [WWW Document]. Seismic Activity. URL https://scweb.cwb.gov.tw/en-us/earthquake/data (accessed 4.20.22).

Sen Gupta, B.K., Machain-Castillo, M.L., 1993. Benthic foraminifera in oxygen-poor habitats. Mar. Micropaleontol. 20, 183–201. doi:10.1016/0377-8398(93)90032-S

Sugawara, D., Minoura, K., Nemoto, N., Tsukawaki, S., Goto, K., Imamura, F., 2009. Foraminiferal evidence of submarine sediment transport and deposition by backwash during the 2004 Indian Ocean tsunami. Island Arc 18, 513–525. doi:10.1111/j.1440-1738.2009.00677.x

Su, C.-C., Huh, C.-A., 2002. 210Pb, 137Cs and 239,240Pu in East China Sea sediments: sources, pathways and budgets of sediments and radionuclides. Mar. Geol. 183, 163–178. doi:10.1016/S0025-3227(02)00165-2

Su, C.-C., Tseng, J.-Y., Hsu, H.-H., Chiang, C.-S., Yu, H.-S., Lin, S., Liu, J.T., 2012. Records of submarine natural hazards off SW Taiwan. Geological Society, London, Special Publications 361, 41–60. doi:10.1144/SP361.5

Tapia, R., Ho, S.L., Wang, H.-Y., Groeneveld, J., Mohtadi, M., 2022. Contrasting vertical distributions of recent planktic foraminifera off Indonesia during the southeast monsoon: implications for paleoceanographic reconstructions. doi:10.5194/bg-2021-329

Uchida, J.-I., Fujiwara, O., Hasegawa, S., Kamataki, T., 2010. Sources and depositional processes of tsunami deposits: Analysis using foraminiferal tests and hydrodynamic verification. Island Arc 19, 427–442. doi:10.1111/j.1440-1738.2010.00733.x

Usami, K., Ikehara, K., Jenkins, R.G., Ashi, J., 2017. Benthic foraminiferal evidence of deep-sea sediment transport by the 2011 Tohoku-oki earthquake and tsunami. Mar. Geol. 384, 214–224. doi:10.1016/j.margeo.2016.04.001

van der Zwaan, G.J., Duijnstee, I.A.P., den Dulk, M., Ernst, S.R., Jannink, N.T., Kouwenhoven, T.J., 1999. Benthic foraminifers: proxies or problems? Earth-Science Reviews 46, 213–236. doi:10.1016/S0012-8252(99)00011-2

van der Zwaan, G.J., Jorissen, F.J., de Stigter, H.C., 1990. The depth dependency of planktonic/benthic foraminiferal ratios: Constraints and applications. Mar. Geol. 95, 1–16. doi:10.1016/0025-3227(90)90016-D

van Hinsbergen, D.J.J., Kouwenhoven, T.J., van der Zwaan, G.J., 2005. Paleobathymetry in the backstripping procedure: Correction for oxygenation effects on depth estimates. Palaeogeography, Palaeoclimatology, Palaeoecology 221, 245–265. doi:10.1016/j.palaeo.2005.02.013

van Marle, L.J., van Hinte, J.E., Nederbragt, A.J., 1987. Plankton percentage of the foraminiferal fauna in seafloor samples from the Australian-Irian Jaya continental margin, eastern Indonesia. Mar. Geol. 77, 151–156. doi:10.1016/0025-3227(87)90089-2

Water Resources Agency – Republic of China, 2022. Water Resources Agency, MOEA [WWW Document]. Water Resources Agency. URL https://eng.wra.gov.tw/ (accessed 4.20.22).

Yamasaki, M., Miyako, S., 2010. Preliminary report of planktic foraminiferal assemblages from surface sediments offwestern Okinawa lslan, in: Arai, K. (Ed.), Marine Geological and Geophysical Studies around Okinawa Islands -Northwestem off of Okinawa Island- Preliminary. p. 175.

10. Tables and Figures

Table 1. Correlation coefficient (Spearman rank) between foraminifera data and environmental parameters. Depth: Water depth (m); %Sand: grain size >63 µm; TOC: TOC content; Temp.: Temperature (ºC) 0–400 m; Sal.: Salinity 0–400 m; Fluo.: Fluorescence 0–400 m; Surface D.O.: Dissolved oxygen 0–400 m; Bottom D.O.: bottom water dissolved oxygen; Planktic: Planktic foraminiferal abundance; Benthic: Benthic foraminiferal abundance.

	Sedimentary			**Hydrography**					**Foraminifera**		
	Depth	**%Sand**	**TOC**	**Temp.**	**Sal.**	**Fluo.**	**Surface DO**	**Bottom DO**	**%P**	**Benthic**	**Planktic**
%P	0.567 ***	-0.199	0.255 *	0.155	0.332 **	-0.488 ***	0.156	-0.354 **	—		
Benthic	-0.650 ***	0.226	-0.389 **	0.107	—	0.250 *	-0.221	0.416 ***	-0.480 ***	—	
Planktic	0.231 *	-0.106	0.098	0.134	0.088	-0.366 **	0.079	-0.126	0.756 ***	0.125	—

Note. * $p < .05$, ** $p < .01$, *** $p < .001$

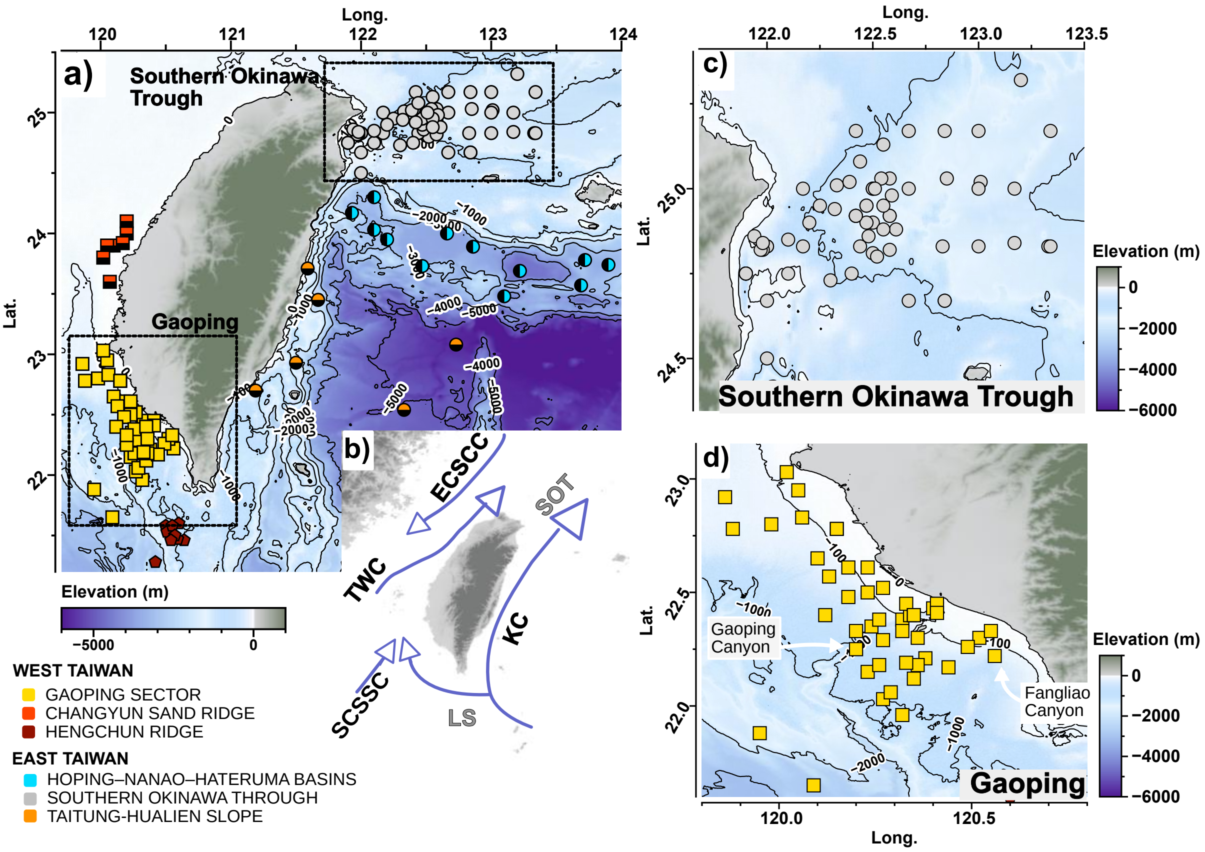

Figure 1. a) Bathymetric chart depicting the location of surface sediment samples analyzed in this study; the inset (b) is a schematic illustrating the location of the Southern Okinawa Trough (SOT) and Luzon Strait (LS) sectors and, the main surface currents offshore Taiwan, namely Kuroshio Current (KC), South China Sea Surface Current (SCSSC), Taiwan Warm Current (TWC) and East Coastal China Sea Current (ECSCC). The study sites were separated into two primary areas according to their longitude, West Taiwan (> 121º E) and East Taiwan (< 121º E). East Taiwan is comprised of the sectors of Southern Okinawa Trough, Hoping-Nanao-Hateruma Basins, and Taitung-Hualien Slope, while West Taiwan is comprised of the sectors of Gaoping, Changyun Sand Ridge, and Hengchun Ridge. Panels (c) and (d) are close-ups of the sectors depicted in (a).

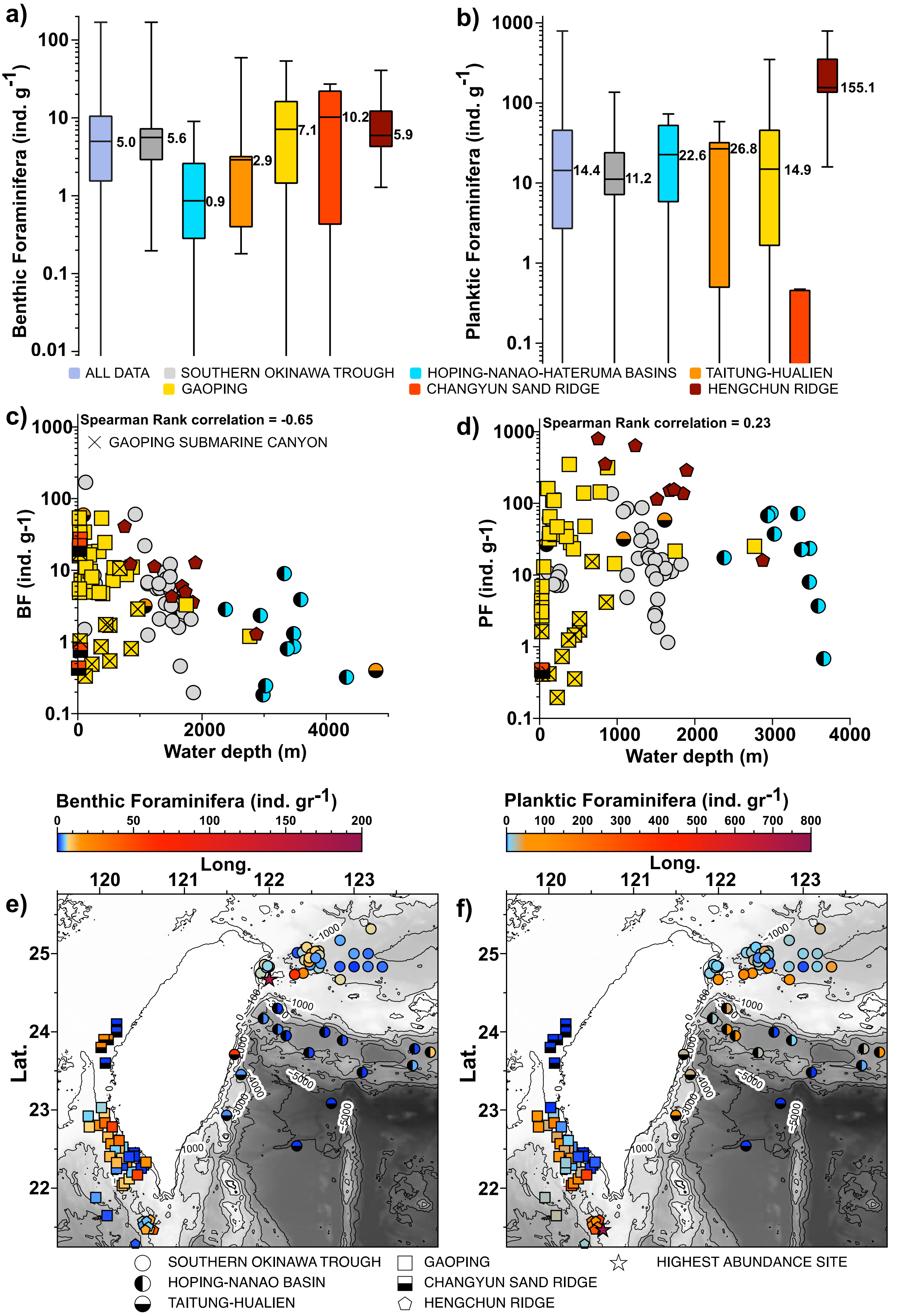

973

974

975 **Figure 2.** Box plots depicting the abundance of benthic (a) and planktic foraminifera (b) (>125 μm)

off Taiwan for the entire dataset and by sectors. In each box plot, whiskers mark the maximum and minimum values, while the number represent the median value. Comparison of the abundances of (c) benthic and (d) planktic foraminifera as a function of bathymetry. Overall, the abundances of benthic foraminifera decrease with depth while the abundances of planktic foraminifera increase. The stations located in the Gaoping and Fangliao submarine canyons are marked (x). The spatial distribution of the abundances of (e) benthic and (f) planktic foraminifera (>125 μm) off Taiwan shows that high abundances of benthic foraminifera are mostly restricted to shallow sites close to the coast while high abundances of planktic foraminifera occur at deep sites. Symbols represent the different sectors considered in this study; stars depict the station with the highest abundance; colors depict the abundance at each site.

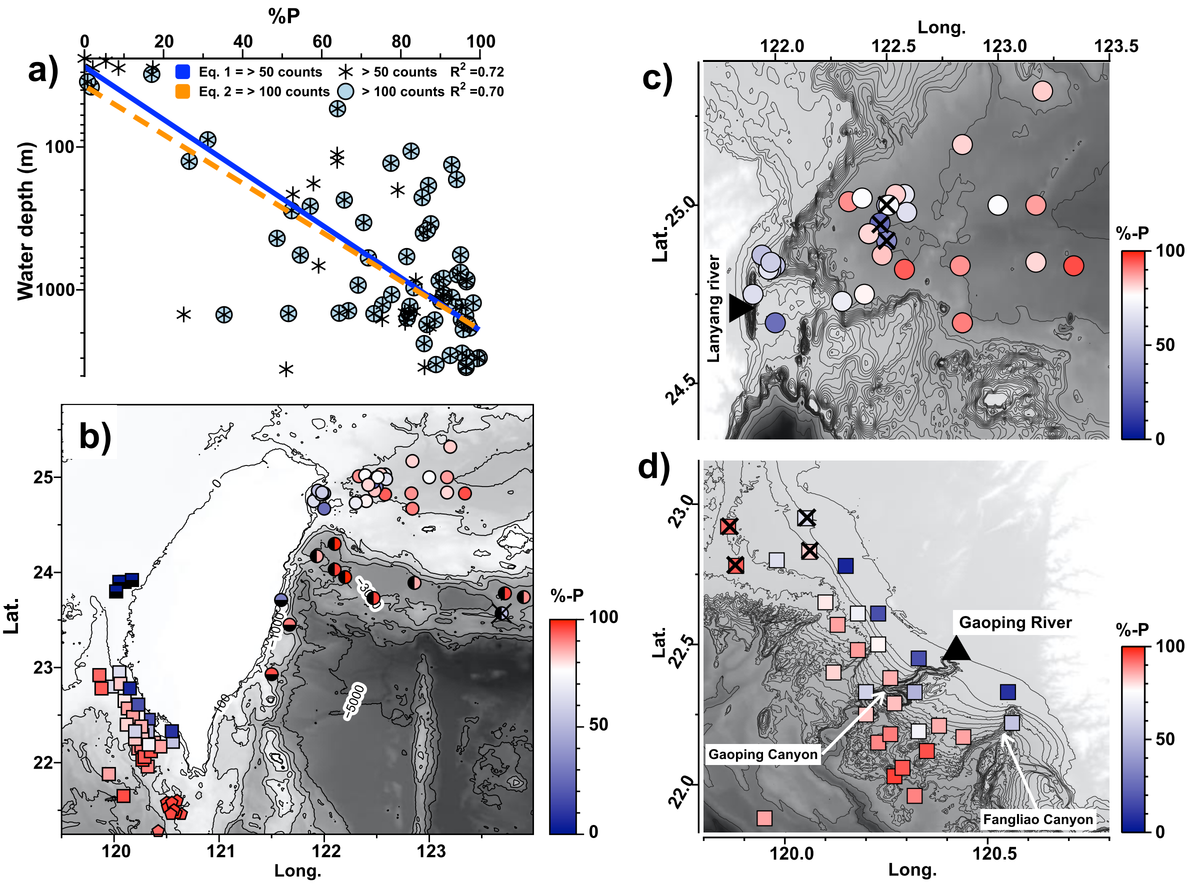

Figure 3. (a) Comparison of the relationship between %P and water depth considering samples with >50 counts (n = 88) (asterisk) and > 100 counts (n = 67) (filled circles). (b) Bathymetric chart off Taiwan showing the spatial distribution of %P values at stations with (a) all >50 foraminifera counts (>125 µm; n = 88), (c) the Southern Okinawa Trough (SOT) and (d) Gaoping sector. Black lines and gray shading depict the seafloor bathymetry; bathymetric lines in c and d show the elevation in 50 m intervals. Stations where %P data lay outside of the 95% prediction range of the regression are marked (x) (see text for details).

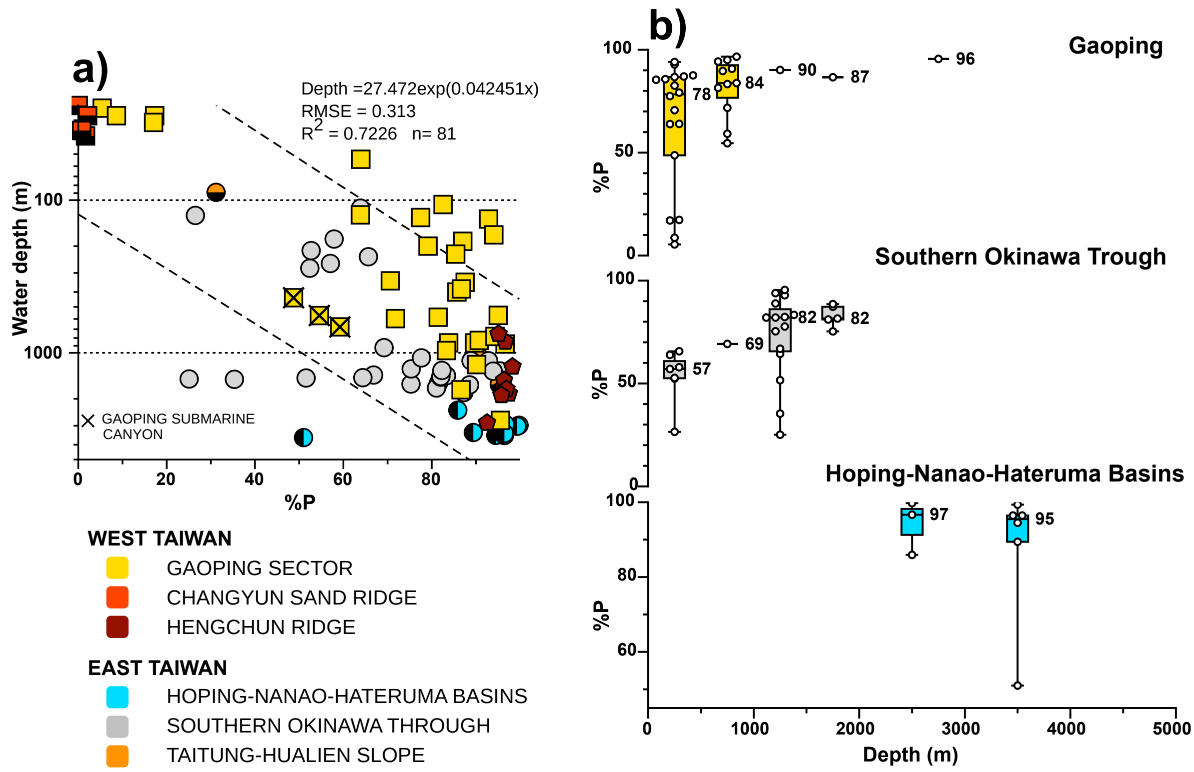

Figure 4. (a) Regression of %P against water depth off Taiwan (n= 81). (b) %P variability by depth range for the sectors of Gaoping (yellow), Southern Okinawa Trough (gray), and Hoping-Nanao Basins (turquoise). The data are grouped by depth bin of 500 m for Gaoping and Southern Okinawa Trough, and 1000 m for Hoping-Nanao-Hateruma Basins. Blue boxes depict the depth bin with the largest data dispersion. The yellow shaded area in (a) depicts the prediction bounds (95%), while stations located in the Gaoping Submarine Canyon are marked by the symbol (x). The numbers in (b) depict the median value for the depth bin.

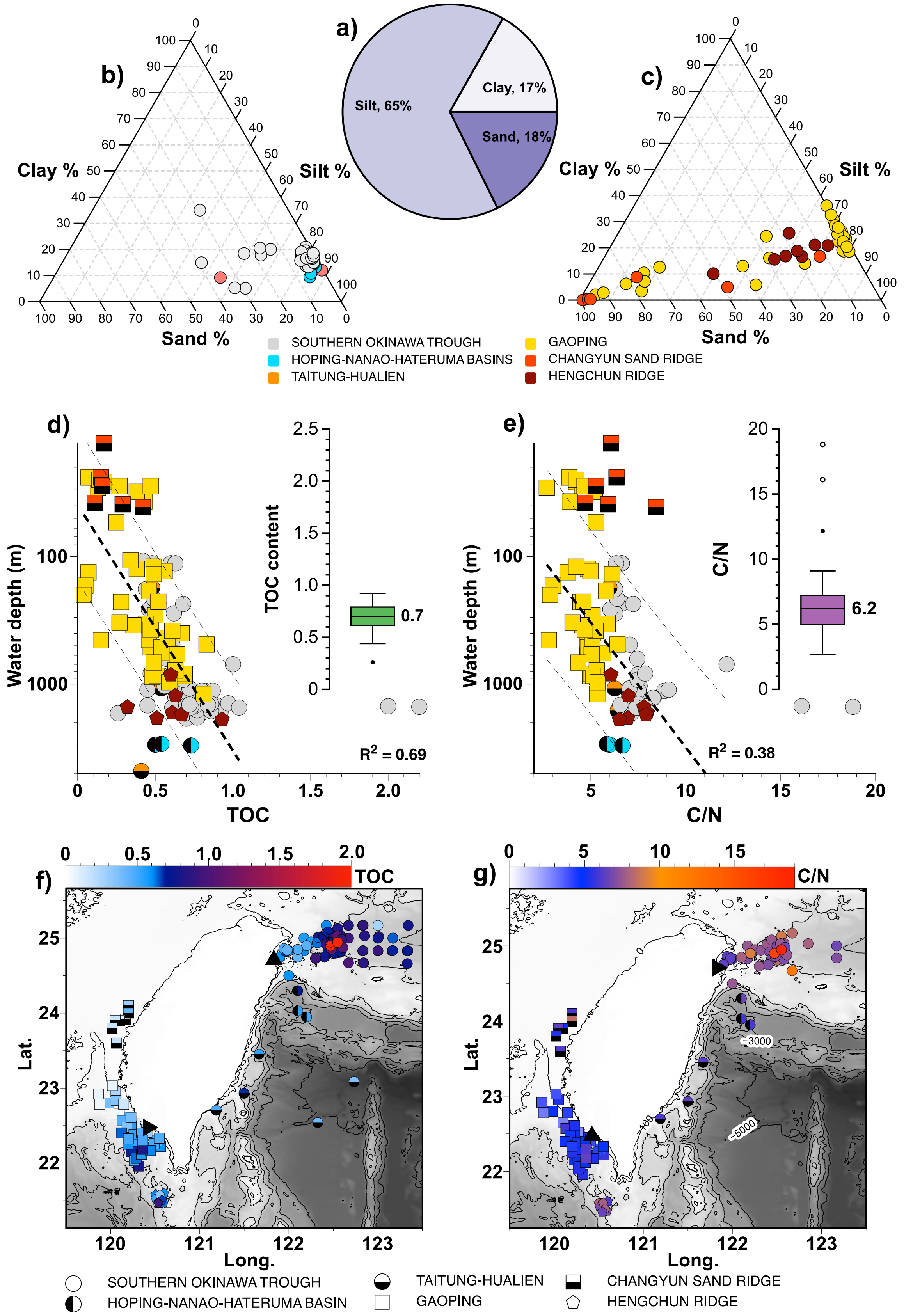

Figure 5. Grain size distribution of (a) the average of the entire dataset off Taiwan, (b) East Taiwan

and (c) West Taiwan. Relationship between water depth and bulk sedimentological parameters, namely (d) Total Organic Carbon (TOC) content and (e) C/N ratio. The TOC content has a stronger correspondence with water depth than C/N. The number in the box plots represents the median value of TOC and the C / N ratio, respectively. Outliers were not considered in the correlation. Open symbols represent sites without data. River mouths i.e., Lanyang (north) and Gaoping (south) are represented by triangles.

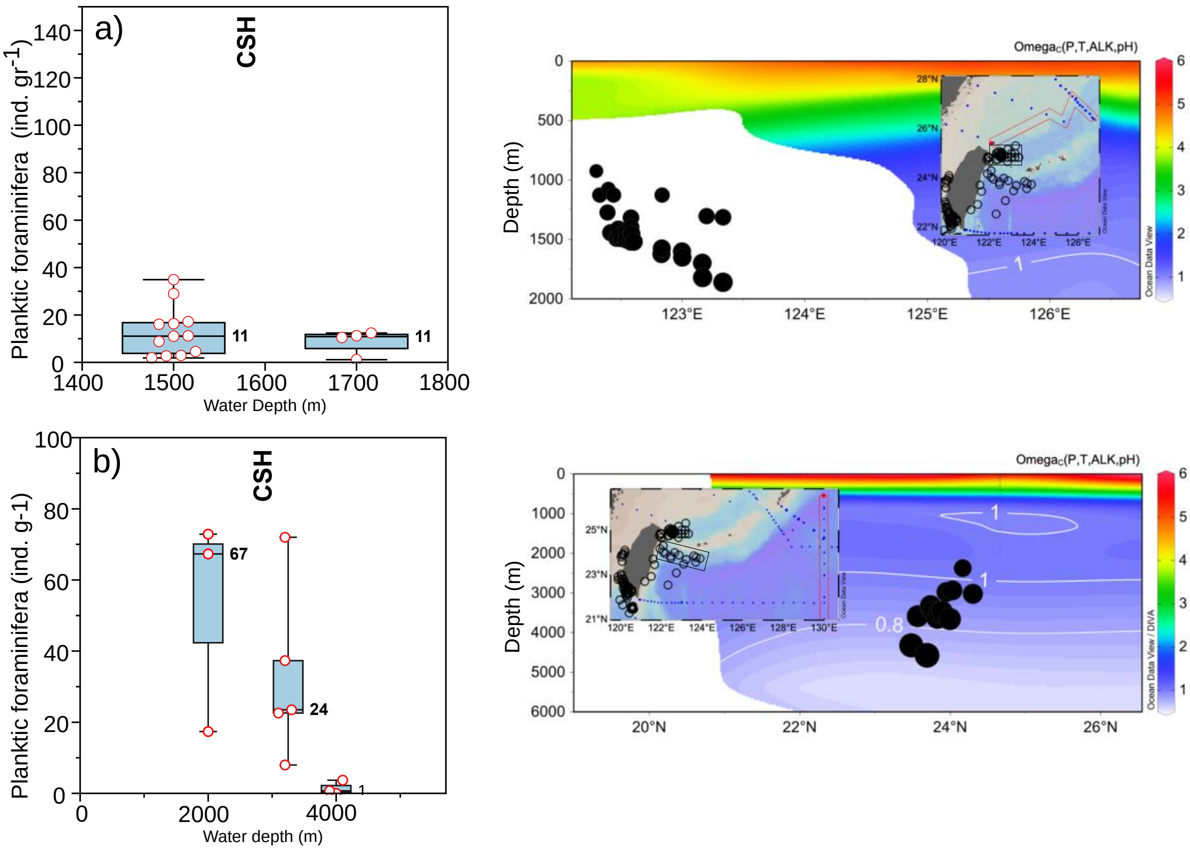

Figure 6. Box plots showing the distribution and average value of foraminifera tests in sediment above and below the Carbonate Saturation Horizon (CSH; $\Omega_c = 1$; indicated by blue shaded bars) for (a) the Southern Okinawa Trough and (b) the Nanao-Hoping-Hateruma Basins. Similar (dissimilar) values above and below the calculated saturation horizon suggest a small (large) effect of carbonate dissolution on the abundance of planktic foraminifera. The Calcite Saturation Horizon was calculated using the GLODAP v.2.2021 database (Olsen et al., 2019) for Ocean Data View (Schlitzer, 2021). The right panels show the oceanographic sections selected for the Calcite Saturation Horizon calculation and the position of the stations in the Southern Okinawa Trough (upper panel) and Nanao-Hoping-Hateruma Basins (lower panel). Red shaded boxes in the insets depict the sectors while the red boxes depict the oceanographic section used in the calculation Ω_c.

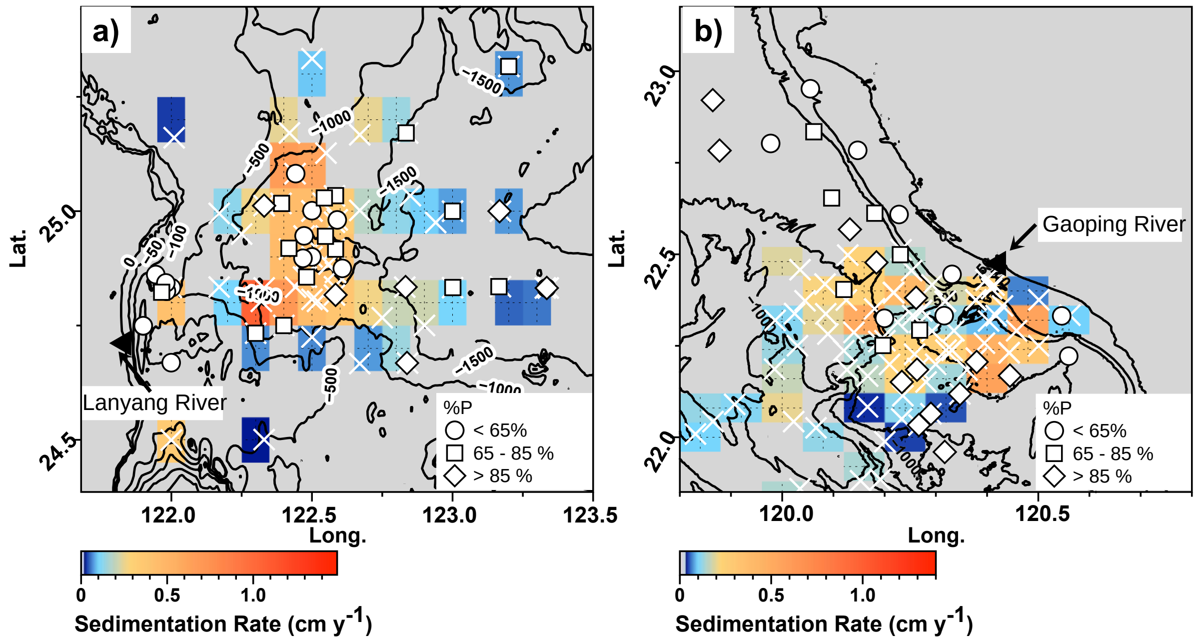

Figure 7. Distribution of %P in (a) Southern Okinawa Trough and (b) Gaoping sectors overlying sedimentation rate estimates based on ^{210}Pb data from Huh et al., 2006, 2009 and Lee et al., 2004. In the Southern Okinawa Trough stations with low (<65%; circles) and moderate (65–85%; squares) %P values concentrate in the sector of high sedimentation rate, while stations with high %P values (>85%) mostly occurs outside of the high sedimentation rate areas. In contrast, in the Gaoping sector, low (<65%; circles) and moderate (65–85%; squares) %P values are associated with the submarine canyons where the sedimentation rates are low due to downslope flushing of sediments. Symbols depict the locations of the %P stations (circle, square, and diamond), ^{210}Pb stations (x), and the Lanyang and Gaoping rivers (triangles).

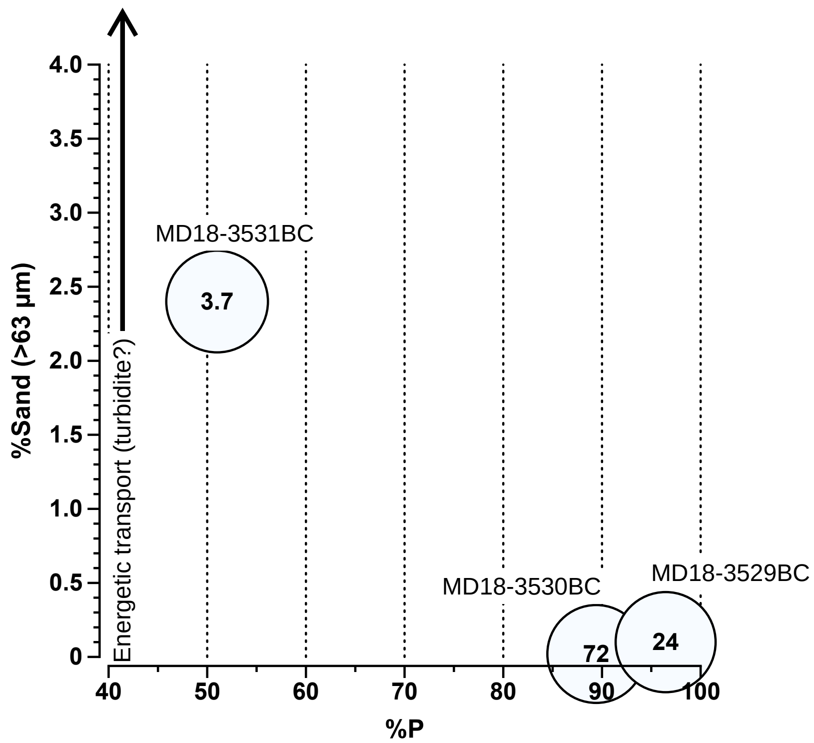

Figure 8. Relationship between %Sand, %P and planktic foraminiferal abundance at three sites in the Hateruma basin. Number in the circles indicate planktic foraminiferal abundance. The %P values at sites MD18-3529BC (3480 m), MD18-3530BC (3326 m), and MD18-3531BC (3590 m) differ substantially despite being located at comparable water depth. The low abundance of planktic foraminifera and high %sand (>63 microns) suggest possible influence of carbonate dissolution as well as the input of allochthonous sediment due to downslope transport (see section 4.3.2 for details).

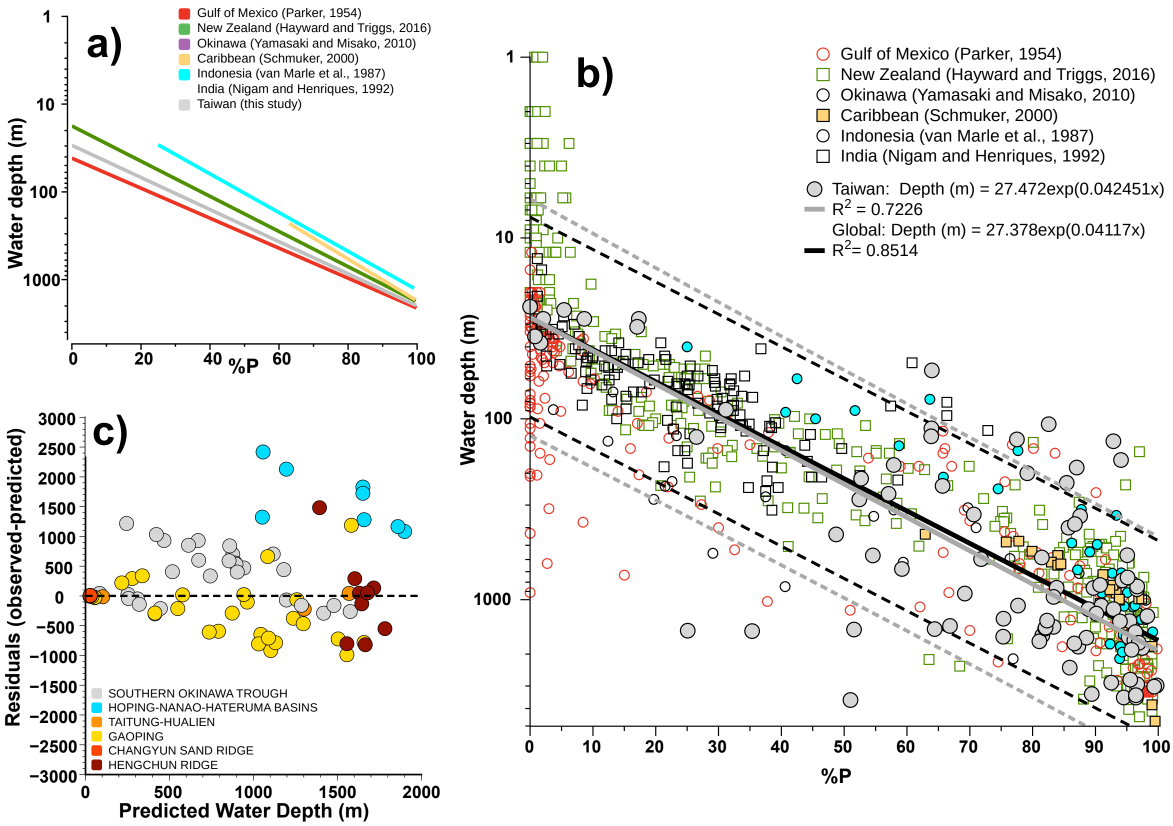

Figure 9. (a) Comparison of the %P-water depth relationship from different regions indicates differences in slope and intercept. (b) All regional datasets show a general positive relationship between %P and water depth albeit with varying degree of scatter. The regression based only on data off Taiwan (n = 81) agrees well with that based on the global compilation (n = 827) obtained by combining all the regional datasets. Solid lines depict the regression equation while the dashed lines depict the 95% prediction bounds. (c) Residuals of the Taiwan calibration show that the bathymetry estimates maybe over- or underestimated by ~1000 m for most sectors.

11. Supplementary Information

Table S1. Details of the core sites used in this study. The sites are divided into East Taiwan that comprises the Southern Okinawa Trough (1), Nanao-Hoping-Hateruma Basins (2), and Taitung-Hualien (3). The area of West Taiwan is consisted of the Gaoping (4), Changchun sand Ridge (5), and Henghun Ridge (6) sectors.

>>> Associated Excel File <<<<<

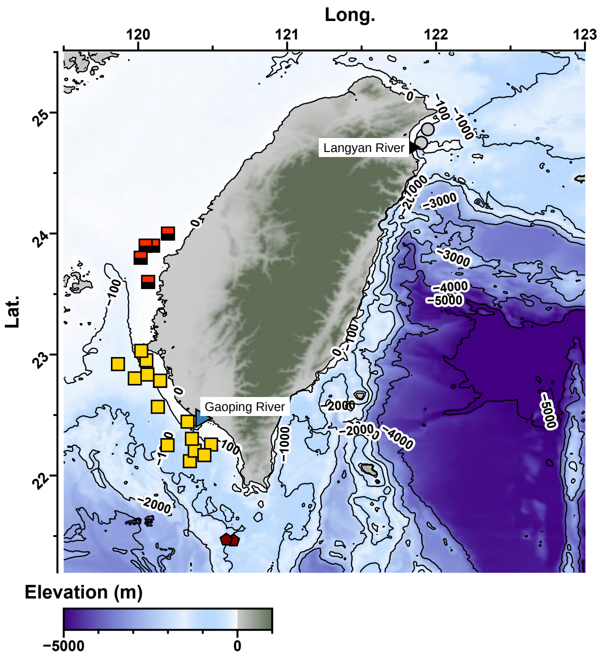

Figure S1. Location of the stations where sediments contain >20% of sand (>63 μm) content. Triangles depict the location of the Lanyang River (black triangle) and Gaoping River (blue triangle).

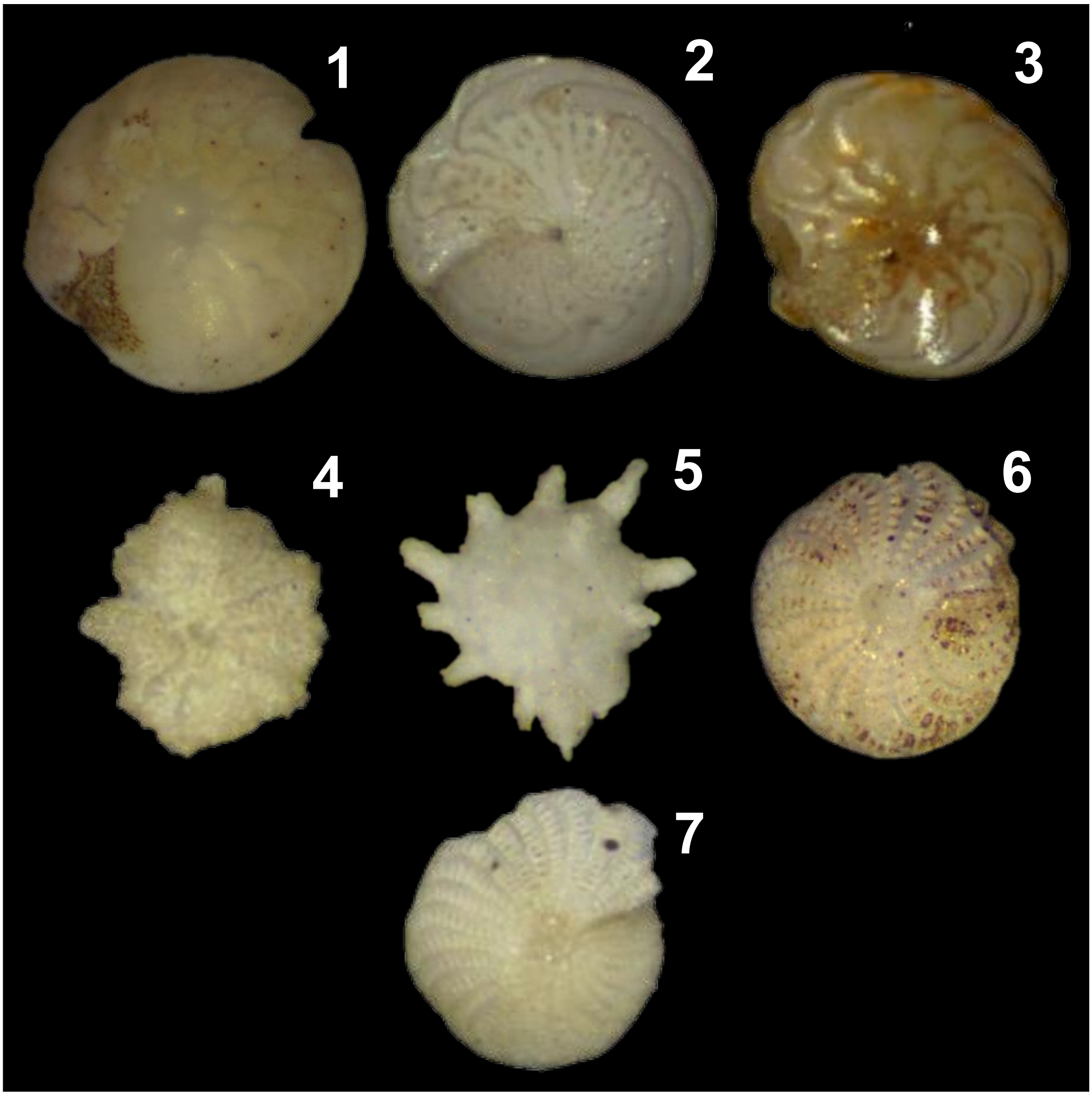

Figure S2. Microphotographs of shallow water benthic foraminifera in the surface sediments of the stations OR1-642-BC22 and OR1-0715-22. *Amphistegina* (1,2,3), *Calcarina* (4), *Neorotalia* (5) and *Elphidium* (6,7).

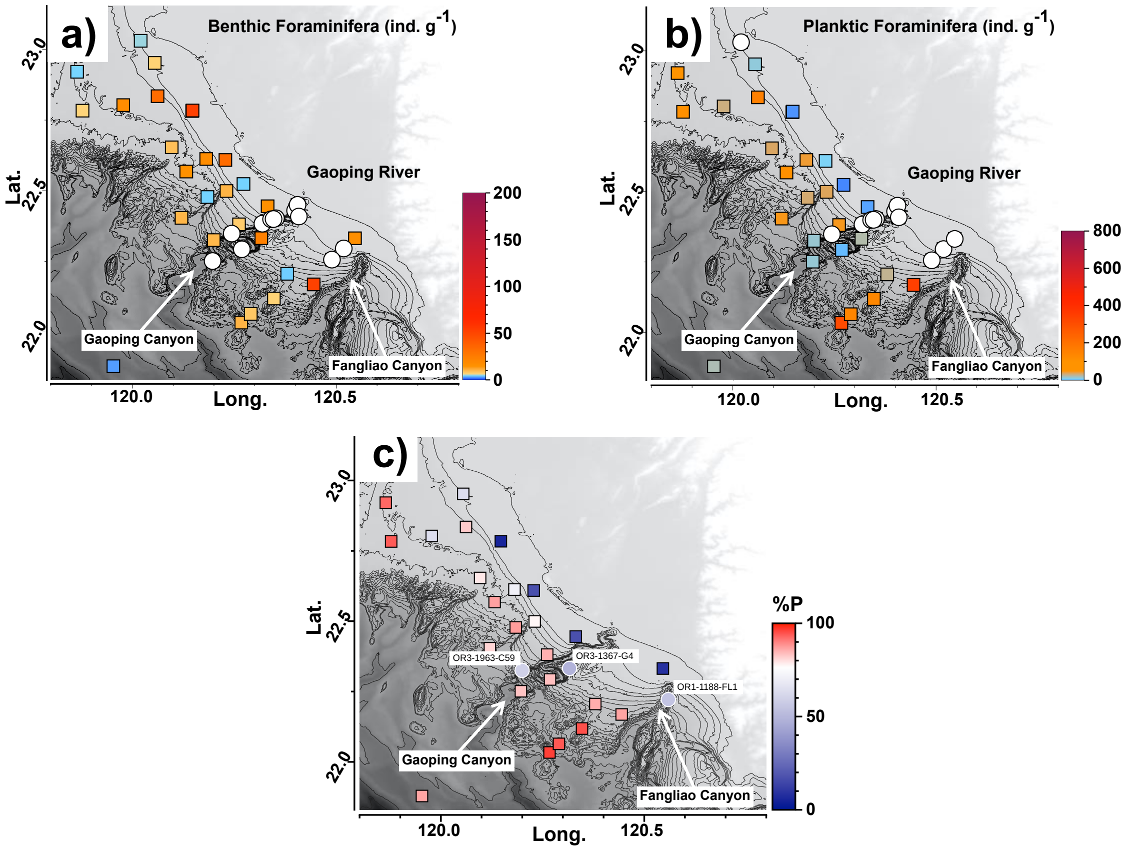

Figure S3. Distribution of (a) benthic and (b) planktic foraminiferal abundance in the Gaoping sector. Sites located in the submarine canyons are characterized by low abundances (< 3 ind. g^{-1}; white circles) while elsewhere the abundances are higher. (c) %P values at sites located in the canyons (circles) are relatively low for their bathymetric range. Black lines and gray shading depict the seafloor bathymetry, and bathymetric lines show the elevation in 50-m intervals.